İZMİR KÂTİP ÇELEBİ ÜNİVERSİTESİ
2010
GRADUATE SCHOOL OF NATURAL AND APPLIED SCIENCES

Determination of the Photodynamic Efficacy on Cancer Cells via Photoelectrochemical Sensors

Submitted to the Graduate School of Natural and Applied Sciences in partial fulfillment of the requirements for the degree of

Master of Science

in Biomedical Engineering

by

Seyedeh Zeinab Mirhosseini

ORCID 0009-0005-1830-2597

Advisor: Assoc. Prof. Nermin Topaloğlu Avşar

July, 2024

This is to certify that we have read the thesis **Determination of the Photodynamic Efficacy on Cancer Cells via Photoelectrochemical Sensors** submitted by **Seyedeh Zeinab Mirhosseini**, and it has been judged to be successful, in scope and in quality, at the defense exam and accepted by our jury as a MASTER'S THESIS.

APPROVED BY:

Advisor: **Assoc. Prof. Nermin Topaloğlu Avşar**
İzmir Kâtip Çelebi University

Co-advisor: **Assoc. Prof. Mustafa Şen**
İzmir Kâtip Çelebi University

Committee Members:

Doç. Dr. Volkan Kılıç
ABD/İzmir Katip Çelebi Üniversitesi

Doç. Dr. İlker Polatoğlu
Manisa Celal Bayar Üniversitesi

Date of Defense: 16.08.2024

Declaration of Authorship

I, **Seyedeh Zeinab Mirhosseini**, declare that this thesis titled **Determination of the Photodynamic Efficacy on Cancer Cells via Photoelectrochemical Sensors** and the work presented in it are my own. I confirm that:

- This work was done wholly or mainly while in candidature for the Master's / Doctoral degree at this university.
- Where any part of this thesis has previously been submitted for a degree or any other qualification at this university or any other institution, this has been clearly stated.
- Where I have consulted the published work of others, this is always clearly attributed.
- Where I have quoted from the work of others, the source is always given. This thesis is entirely my own work, with the exception of such quotations.
- I have acknowledged all major sources of assistance.
- Where the thesis is based on work done by myself jointly with others, I have made clear exactly what was done by others and what I have contributed myself.

Date: 16.08.2024

_____

Determination of the Photodynamic Efficacy on Cancer Cells via Photoelectrochemical Sensors

Abstract

Photodynamic Therapy (PDT) represents a promising alternative to traditional cancer treatments, leveraging the action of reactive oxygen species (ROS) to target tumors while minimizing damage to surrounding healthy tissues. This study investigates the photodynamic efficacy of Chlorin e6 (Ce6)-mediated PDT on SKOV-3 ovarian cancer cells, utilizing a 655-nm diode laser. The primary objectives were to evaluate cell viability, intracellular ROS production, and ROS generation capacity using fluorescence-based assays and electrochemical sensors, particularly screen-printed electrodes (SPEs).

The results demonstrated that exposure to 25 J/cm² of laser light did not significantly impact SKOV-3 cell viability. However, a combination of Ce6 and PDT resulted in a substantial reduction in cell viability, particularly at higher Ce6 concentrations. The production of ROS, crucial for the effectiveness of PDT, was confirmed through the increased fluorescence intensity of the DCFH-DA probe and reduced absorbance in DPBF assays. The electrochemical analysis further validated the concentration-dependent and power-dependent generation of ROS.

These findings highlight the potential of Ce6-mediated PDT as a therapeutic strategy for ovarian cancer. The use of SPEs for real-time monitoring of ROS production offers a sensitive and cost-effective method to optimize PDT protocols, enhancing therapeutic outcomes while minimizing adverse effects. This study underscores the significance of precise ROS detection in improving the efficacy of photodynamic therapy.

Keywords: Photodynamic Therapy, Reactive Oxygen Species, Chlorin e6, Screen-Printed Electrodes, Hydroquinone, SKOV-3 Cells.

Kanser Hücreleri Üzerindeki Fotodinamik Etkinliğin Fotoelektrokimyasal Sensörlerle Belirlenmesi

Öz

Fotodinamik Terapi (PDT), tümörleri hedef almak için reaktif oksijen türlerinin (ROS) etkisini kullanarak çevredeki sağlıklı dokulara zarar vermeyi en aza indirirken, geleneksel kanser tedavilerine umut verici bir alternatif sunmaktadır. Bu çalışma, SKOV-3 over kanser hücrelerinde Chlorin e6 (Ce6) aracılı PDT'nin fotodinamik etkinliğini 655 nm diyot lazer kullanarak araştırmaktadır. Ana hedefler, hücre canlılığını, hücre içi ROS üretimini ve ROS'un hem floresan bazlı testler hem de özellikle baskı devreli elektrotlar (SPE'ler) kullanılarak elektrokimyasal sensörlerle üretim kapasitesini değerlendirmektir.

Sonuçlar, 25 J/cm² lazer ışığına maruz kalmanın SKOV-3 hücre canlılığı üzerinde önemli bir etki yaratmadığını göstermiştir. Bununla birlikte, Ce6 ve PDT kombinasyonu, özellikle daha yüksek Ce6 konsantrasyonlarında, hücre canlılığında önemli bir azalmaya yol açmıştır. PDT'nin etkinliği için kritik öneme sahip olan ROS üretimi, DCFH-DA probunun artan floresan yoğunluğu ve DPBF testlerinde azalan absorbans ile doğrulanmıştır. Elektrokimyasal analiz, ROS üretiminin konsantrasyona ve güce bağlı olarak gerçekleştiğini daha da doğrulamıştır.

Bu bulgular, Ce6 aracılı PDT'nin over kanseri için terapötik bir strateji olarak potansiyelini vurgulamaktadır. ROS üretiminin gerçek zamanlı izlenmesi için SPE'lerin kullanımı, PDT protokollerini optimize etmek için hassas ve maliyet etkin bir yöntem sunarak terapötik sonuçları iyileştirirken olumsuz etkileri en aza indirmektedir. Bu çalışma, fotodinamik terapinin etkinliğini artırmada hassas ROS tespitinin önemini vurgulamaktadır.

Anahtar Kelimeler: Fotodinamik Terapi, Reaktif Oksijen Türleri, Klorin e6, Ekran Baskılı Elektrotlar, Hidrokinon, SKOV-3 Hücreleri

Acknowledgment

I would like to express my deepest gratitude to all those who have supported and guided me throughout the course of my thesis work.

First and foremost, I am profoundly grateful to my advisor, Assoc. Prof. Nermin Topaloğlu Avşar for their invaluable guidance, insightful feedback, and unwavering support. Their expertise and encouragement have been instrumental in the completion of this research.

I am equally grateful to my co-advisor, Assoc. Prof. Mustafa Şen for their continuous support, encouragement, and valuable insights. Your dedication and advice have significantly contributed to the success of this work.

I extend my heartfelt thanks to the members of my thesis committee, Doç. Dr. Volkan Kılıç and Doç. Dr. İlker Polatoğlu for their constructive critiques and thoughtful suggestions. Your contributions have significantly enhanced the quality of this work.

I would also like to acknowledge the Electrochemical Biosensor for providing the resources and facilities necessary for my research. Special thanks Tuğba Akkaş for their assistance and cooperation.

My appreciation goes to my fellow students and friends, particularly Research Assistant Büşra Sirek for their camaraderie and for creating an inspiring and collaborative environment. Your support and shared enthusiasm have been a great source of motivation. I am also deeply thankful to my friends, Şerife Özcan and Nisa Celebi for their steadfast support and encouragement.

A special thank you to my family for their endless encouragement, patience, and understanding. Your love and support have been a constant source of strength throughout this journey. Finally, Most importantly, I would like to express my heartfelt gratitude to my husband, Sait for his unwavering support, understanding, and love. Your encouragement and belief in me have been vital in completing this thesis. Thank you all for being an integral part of this achievement.

Table of Contents

List of Figures

List of Abbreviations

$^1O_2$	Single oxygen
BQ	Benzoquinone
CA	Chronoamperometry
Ce6	Chlorin e6
CO_2	Carbon Dioxide
DMSO	Dimethyl Sulfoxide
DPV	Differential Pulse Voltammetry
FBS	Fetal Bovine Serum
HQ	Hydroquinone
J/cm^2	Joules per Square Centimeter
MTT	3-(4,5-Dimethylthiazol-2-yl)-2,5-Diphenyl Tetrazolium Bromide
PBS	Phosphate Buffered Saline
PDT	Photodynamic Therapy
ROS	Reactive Oxygen Species
SD	Standard Deviation
SKOV-3	Human Ovarian Cancer Cell Line
SPE	Screen-Printed Electrodes

List of Symbols

CO_2	Carbon Dioxide
^0C	Celsius Degree
G_1	Gap 1
G_2	Gap 2
H_2O_2	Hydrogen Peroxide
$\cdot OH$	Hydroxyl Radical
O_2	Oxygen
$^1O_2$	Singlet Oxygen
$\cdot O^{2-}$	Superoxide Radical
$(O_2\bullet-)$,	superoxide
$(HO_2\bullet)$,	hydroperoxyl
$(\bullet OH)$,	hydroxyl
$(ROO\bullet)$,	peroxy
$(RO\bullet)$	alkoxy
$(^1O_2)$.	singlet oxygen

Chapter 1

Introduction

Cancer has been a leading cause of death, representing a major global health issue and causing millions of deaths annually. Conventional treatment options traditionally include surgery, chemotherapy, and radiation therapy, which have serious limitations on people's quality of life. Despite novel agents for the treatment of different types of cancer, these conventional methods cause side effects that can be severe and malignant. Over time, the solution has evolved into a new and more tolerable therapy.

Photodynamic Therapy (PDT) is an option where photosensitizers, which are light-sensitive drugs, are used. The photosensitizing mechanism of these pharmacophores is the induction of a specific light wavelength-driven formation of reactive oxygen species (ROS), a group of highly reactive molecules that can cause apoptosis in irradiated cells. In PDT, the production and location of ROS are considered essential indicators for determining efficacy for successful treatment.

One of the important mechanisms of PDT is interrupting the ROS defense line. Upon light activation, photosensitizers transfer energy to surrounding oxygen molecules, converting them into reactive oxygen species (ROS), including singlet oxygen, superoxide radicals, and hydroxyl radicals. ROS causes damage to cellular macromolecules such as lipids, proteins, and DNA, which results in the death of cancer cells. It is important to confirm the reliable detection of ROS so that we can monitor and improve PDT therapeutics for generating enough ROS. At the same time, We make a key effort to detect ROS that will be experimented on by applying commercially available kits for determination in biological environments. These kits are usually based on fluorescent or colorimetric assays in which ROS reacts with dedicated probes, recapitulating a measurable signal. However, these probes offer specificity, sensitivity, and stability, but these assays are subject to interference from the complex biological environment, which can compromise their accuracy, rendering inaccurate results.

In this regard, electrochemical sensors have emerged as an alternative for the detection of ROS, and screen-printed electrodes (SPEs)--based biosensors offer effective solutions to perform this experiment. Electrochemical sensors create electrical signals from chemical reactions that can be measured and quantified. SPEs are attractive due to their easy methodologies, low costs of fabrication, real-time measurements, and portable nature. These sensors can be easily tuned to be highly sensitive and selective towards certain analytes such as ROS using nanomaterial modification. Due to the light activation, ROS originated by photosensitizers could be detected electrochemically and indicate real-time monitoring of ROS generation for the optimization of PDT efficacy. This ensures accurate monitoring and optimization of PDT protocols and may contribute to better therapeutic results.

PDT offers a promising alternative to traditional cancer treatments by using the action of reactive oxygen species (ROS) to specifically target tumors while minimizing damage, thereby overcoming the limitations associated with current regimens. The precise detection of ROS is indispensable to enhance the therapeutic efficacy of PDT. Even though conventional ROS detection kits have restrictions, there is still a simplistic and powerful way to detect the existence of ROS in different samples by using electrochemical sensors, especially SPEs. It could bring a big leap in PDT monitoring and efficacy for cancer therapy.

1.1 Cancer

These diseases are complicated; this holds for cancer, which is riddled with multiple challenging problems in many ways. Cancer is characterized by uncontrolled cell growth that leads to the formation of large tumors, causing surrounding tissues to become damaged rapidly and resulting in life-threatening conditions. Cancer is usually initiated when genetic mutations substantially disrupt the finely-tuned process of cell growth and division. Cancer is a complex biological process; it is not just a disease. Fighting such a battle poses significant health and life challenges for those who suffer from it. How it acts, together with its significant impacts, needs to be examined through insights gathered from clinical and essential sciences. Cancer affects tissues and organs, both nearby and distant in our body, causing disturbances that sometimes reach throughout the whole organism, creating paraneoplastic syndromes. These

syndromes are a human enigma and have also been described in various species of domestic or wild animals. These results suggest that secondary cancer events are at least as important as the primary tumor and that elucidating these consequences is a highly interdisciplinary task that requires input from both clinical and basic science research [1].

Physicians and surgeons have observed how cancer behaves in human cases over centuries, leading to an increased understanding of cancers. Our development of understanding has been slow, and much new information on other animal species and plants has only recently become apparent. We now know, with modern research tools, that cancers in other species have at least some superficial similarities with human cancers, but there are also important differences, and it is unwise to simply extrapolate from one species to another. These malignant characteristics include their relatively low dependence on growth factors, ability to proliferate in an anchorage-independent manner, loss of contact inhibition, and so forth. Control of the cell cycle and, hence, regulation of DNA replication and cell division are frequently disrupted in cancer cells by mutations in genes normally required for the cell cycle [2].

The cell cycle is one of the basic phenomena where a cell grows, duplicates its DNA, and divides into two daughter cells. G1 (gap 1), S (synthesis), G2 (gap 2), and M (mitosis) are four different phases of the cell cycle. (Figure 1.1) DNA replication and cell division are exquisitely controlled in each phase again for proper DNA replication advocacy. As you can see from these 4 stages namely the G1 phase (cell growth and preparation for DNA synthesis), S phase (DNA replication), G2 phase (further growth and preparation for mitosis), and M phase of the cell cycle many things are happening for a single mother cell to divide into two daughter cells by mitosis followed by cytokinesis. Pregnant CDK protein, by binding to cyclins and forming a complex, regulates the transition between different phases of mitosis activating or inactivating target proteins by phosphorylation. Cellular checkpoints at specific stages of the cell cycle, including the G1/S checkpoint, G2/M checkpoint, and spindle assembly checkpoint, assess genome integrity and the fate of critical events. Indeed, the G1/S checkpoint prevents cells from replicating their DNA while there are insufficient building blocks for making new DNA and the proper health of existing DNA chemicals to participate in propelling the process forward; the G2/M checkpoint

confirms that everything is ready so it is good time to go ahead with mitosis since all damaged or unreplicated parts of nuclear/DNA architecture have been dealt with properly. The SAC monitors chromosome congression and only permits the partitioning of chromosomes to opposite spindle poles once all chromosomes have established bipolar tension. Dysregulation of such regulatory mechanisms occurs commonly in cancer and results in uncontrolled cell growth. Dysregulation of the latter is driven by crucial mutations in tumor suppressors (e.g., TP53, RB1) and oncogenes (e.g., MYC, RAS) [5]. As such, therapeutic strategies to correct the cell cycle dysregulation will be important in this setting. For example, CDK inhibitors seek to retain control over the cell cycle and arrest/release of the cells in the G1 phase or promote apoptosis when appropriate. Moreover, there are investigations into targeted systems related to centrosome amplification and spindle assembly checkpoint defects for the treatment of cancer [3, 4] (Figure 1.1).

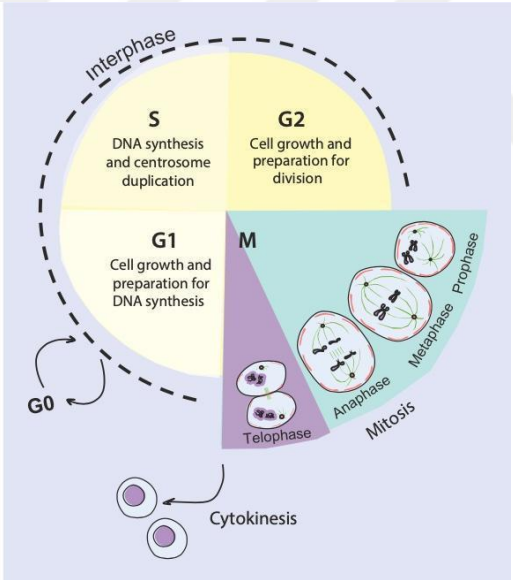

Figure 1.1: The Cell Cycle [5]

Oxidative stress can vary from senescence to apoptosis or transformation and depends on many variables, which include intracellular conditions (mostly ROS generation and the balance between the generation of free radicals on one hand and antioxidant defenses on the other) [5]. In cells, mitochondria represent the major organelle that produces reactive oxygen species (ROS), with ROS generated by the overactive electron transport chain being particularly crucial. Considering that cancer cells often suffer from mitochondrial dysfunction and metabolic reprogramming, which, in turn, results in a larger quantity of reactive oxygen species (ROS). Although excess ROS is

generally toxic to normal cells, cancer cells respond by increasing antioxidant pathways that reduce or quench the levels of signaling ROS and serve in a pro-survival manner. Adaptation is achieved by enabling cancer cells to convert the signaling of reactive oxygen species (ROS) into a survival and proliferation advantage. ROS are known to be second messengers in many signal transduction pathways, and they contribute to malignant proliferation pathways [6]. ROS also activates the PI3K/Akt signaling pathway by inactivating its inhibitors, which are protein tyrosine phosphatases like PTEN. This pathway plays an essential role in cell survival and growth. On the other hand, ROS can activate MAPK and Src kinase pathways, leading to increased cellular signaling for carcinogenesis. This generates a feedforward loop for ROS production and synthesis of signal molecules, which promotes tumor development [8].

Furthermore, ROS contributes to the tumor microenvironment (TME), which is frequently hypoxic in solid tumors. Reactive oxygen species (ROS) are induced in response to hypoxia and lead to the stabilization of hypoxia-inducible factors (HIFs), which regulate multiple genes involved in angiogenesis, metabolism, and cell survival. This response facilitates the ability of tumors to adapt to hypoxic conditions and enhances their growth and metastatic capacity [8, 6].

1.1.1 Ovarian Cancer

The ovaries are paired, almond-shaped organs located on either side of the uterus within the female reproductive system. They play a critical part in reproduction and hormone production. The main purpose of the ovaries is to produce hormones, which change during puberty. As levels of gonadotropin-releasing hormone rise, the ovaries release estrogen, testosterone, inhibin, and progesterone (Figure 1.2) [16]. Each ovary consists of an outer cortex and an inner medulla. Many follicles at various stages of growth are found in the cortex. Each follicle houses an immature egg, which matures when signaled by hormone levels throughout the menstrual cycle. When the egg matures, it is released from the ovary during ovulation, which usually happens in the middle of the menstrual cycle. The medulla comprises blood vessels, nerves, and supporting tissues. It supports the metabolic processes of the ovary and facilitates the passage of hormones and growth factors needed for ovarian function [17].

In the United States and Northern Europe, there is a significant burden of ovarian cancer, resulting in 13,770 women dying from the disease in 2021. It is most commonly seen in the United States and Northern Europe and least common in Africa and Asia. Ovarian cancer is the ninth most common cancer among women and ranks seventh in mortality, accounting for 3% of all malignancies diagnosed [12]. Derived from a very late stage, it has few therapeutic resources to rely on and fairly low overall survival rates [14]. Ovarian cancer usually occurs in older people and is often not present in family history, although some women inherit the risk from previous generations. There is growing evidence that hysterectomy and tubal ligation for sterilization significantly reduce the risk of ovarian cancer, and this corresponds with a high proportion of women whose families are not at risk and a reduced overall risk in places where childbearing is common. The evidence on other factors such as hormone replacement therapy, fertility medicine treatment, breastfeeding, and infertility is inconclusive [13]. Classification of ovarian tumors is primarily based on the area of the ovary from which they originate, including the epithelium (which includes the outer mesothelial layer), stroma, and germ cells [15].

There are two types of epithelial ovarian cancers: Type I and Type II. Type I cancers, including low-grade serous, endometrioid, clear cell, and mucinous forms, demonstrate localized growth and late metastasis, with associations to endometriosis. They are often found in the fallopian tube or on the ovarian epithelium. Serous carcinoma, carcinosarcoma, and undifferentiated carcinoma are examples of Type II malignancies characterized by high invasiveness and a tendency to be diagnosed at advanced stages. These cells usually arise from highly malignant abnormalities in the fallopian tubes, become cancerous, and spread rapidly throughout the peritoneal cavity [12].

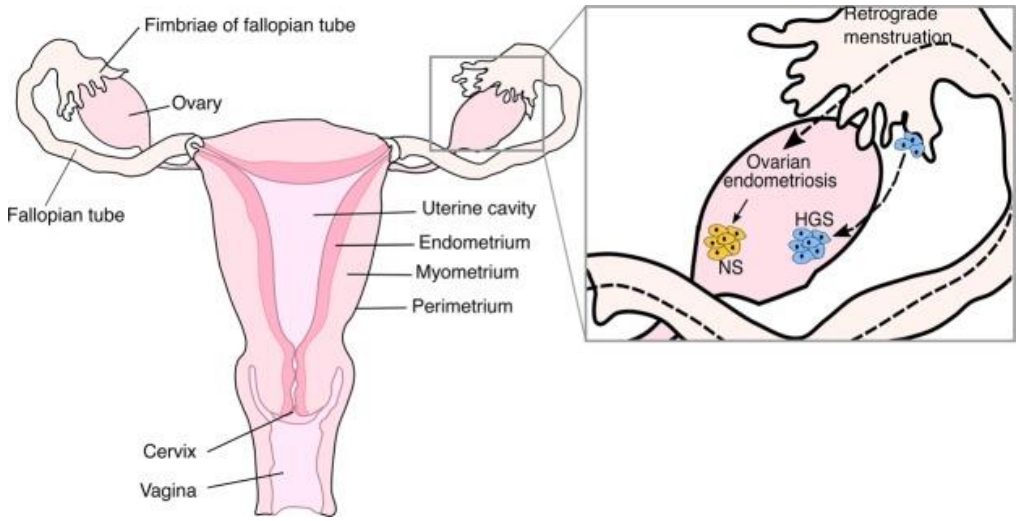

Figure 1.2: Anatomy of the female reproductive system and cancer biology of the ovary [78].

1.1.2 Conventional Treatments

Cancer treatments usually involve surgery, radiation, and systemic therapy using hormone drugs, chemotherapy, or targeted biological therapies alone or in combination [18]. Cancer treatments usually involve surgery, radiation, and systemic therapy using hormone drugs, chemotherapy, or targeted biological therapies, either alone or in combination [19].

Ovarian cancer can be diagnosed through a pelvic examination or ultrasound. The stage of ovarian cancer is determined by the degree of metastasis from its primary site [12]. FIGO is responsible for setting up the staging recommendations for ovarian cancer. Precise classification using IBM must be performed for accurate staging, which is necessary not only for prognosis, therapy, clinical trial execution, and adequate communication. Surgical staging is used to categorize ovarian cancer, and confirmation of the diagnosis occurs during surgery once the ovary has been removed. Ovarian cancer is a malignant entity arising from the fallopian tube and the peritoneum. These cancers are grouped due to their common cell origin, ovary involvement, and the fact that they should all be treated in the same way. Ovarian malignancies are classified based on the histologic component of the ovary, and epithelial ovarian cancer is the leading cause of gynecological cancer death in the United States and Europe [23]. Treatment in early-stage ovarian cancer is based on the stage of the disease and the extent of cytoreduction. Up to 25% of women have some

sort of finding in one or both ovaries or pelvic region. Surgical, chemotherapy and investigational treatments are available. This surgery may include a total hysterectomy (removal of the uterus), bilateral salpingo-oophorectomy (removal of both fallopian tubes and ovaries), partial omentectomy, and examination of lymph nodes or tissues in the body for classification and staging purposes. Patients with stage IA or B disease, usually grade 1 and occasionally grade 2, are administered chemotherapy. Platinum-based chemotherapy is used in patients at high risk There are also clinical trials for chemotherapy, radiotherapy, as well as targeted molecular therapy. A study comparing adjuvant chemotherapy with platinum versus observation after surgery found, respectively, 0.64 and 0.67 hazards for recurrence-free survival (RFS) and overall survival. Effect of 3 vs 6 cycles of adjuvant paclitaxel and carboplatin on relapse-free survival among women with early-stage ovarian cancer: A randomized clinical trial. They found a marked reduction in the odds of cancer coming back (24%) within five years. Of course, the OS was similar for both treatment regimens and there was no significant difference in reducing recurrence [21, 24].

After surgery for most ovarian cancers, especially those in more advanced stages, chemotherapy is the standard treatment. Chemotherapy regimens often include platinum-containing drugs such as carboplatin and paclitaxel [22]. These medicines help suppress any remaining cancer cells and prevent the disease from coming back. Chemotherapy is typically administered in cycles, with a common regimen consisting of six cycles, with a three-week interval between each cycle. Neoadjuvant chemotherapy (NACT) is employed when immediate surgery cannot be performed, with the hope of downsizing the tumor prior to surgery. This approach may limit surgical morbidity and is as effective as initial surgery [25]. They also offer intraperitoneal chemotherapy, where the drugs are placed directly into the abdominal cavity, which has been shown to have a much better effect on remaining cancer cells. Nevertheless, there are many side effects related to the use of chemotherapy, such as nausea, vomiting, alopecia, fatigue, neuropathy, myelosuppression (decreased activity of the bone marrow), and increased infections. In the long run, these agents can cause nephrotoxicity and irreversible sensorineural hearing loss, with platinum compounds being more prevalent [26]. They also offer intraperitoneal chemotherapy, where the drugs are placed directly into the abdominal cavity, which has been shown to have a much better effect on remaining cancer cells. Nevertheless, there are many side effects

related to the use of chemotherapy, such as nausea, vomiting, alopecia, fatigue, neuropathy, myelosuppression (decreased activity of the bone marrow), and increased infections. In the long run, these agents can cause nephrotoxicity and irreversible sensorineural hearing loss, with platinum compounds being the most prevalent [12].

They also offer intraperitoneal chemotherapy, where the drugs are placed directly into the abdominal cavity, which has been shown to have a much better effect on remaining cancer cells. Nevertheless, there are many side effects related to the use of chemotherapy, such as nausea, vomiting, alopecia, fatigue, neuropathy, myelosuppression (decreased activity of the bone marrow), and increased infections. In the long run, these agents can cause nephrotoxicity and irreversible sensorineural hearing loss, with platinum compounds being the most common culprits [27]. Although different treatment modalities are highly effective in ovarian cancer management, they carry a range of side effects that should be managed properly to balance patient quality of life and treatment effectiveness. Recognizing these potential side effects is an important aspect of creating individualized treatment plans [24, 27].

1.2 Photodynamic Therapy

Laser technology has had a profound impact on many aspects of science and medicine, providing powerful tools for diagnostic purposes, therapy, and surgery [28]. Using a ruby crystal, Theodore Maiman created the first working laser in 1960. The unique characteristics of laser light, including coherence, monochromaticity, and directionality, make it indispensable for present-day medical applications. Lasers have come a long way since then, and today there are many different types of lasers, each with unique characteristics that make them ideal for various medical conditions [30].

Phototherapy, or heliotherapy, was quite common in ancient times when beams of light were believed to be a God-given cure for conditions such as vitiligo, psoriasis, rickets, skin cancer, and psychosis. However, as science advanced, it became understood that endogenous substances were the actual cure, and a phototherapeutic mechanism for their pharmacological action became a better possibility [31]. Phototherapy has a history spanning from Ancient Egypt and India around 3000 BC, where Egyptians

used a powder of photosensitizing plants such as Ammi majus, parsnip, parsley, and Saint-John's-wort to apply on depigmented lesions [32].

It was essentially a religious practice in China during the Tang dynasty, people left green paper out with red dye to soak up sunlight and then ate it as they believed by doing so would be able to draw the sun's powerful healing forces. The "Father" of medical science, Greek doctor Hippocrates was the first to advise sunlight for health regeneration. The Romans, however, did treat skin disease with sunlight and this continued to be used but during the decline of The Roman Empire and the growth of Christianity the Roman baths were dismantled and heliotherapy as a concept disappeared [33].

In the late 1800s and early 1900s, Swiss naturopath Arnold Rikli reintroduced the healing power of sunlight, which had been forgotten for centuries. He founded a national medical institute in Slovenia and worked on the development of natural remedies that are still valid today. Niels Ryberg Finsen, a Danish doctor, used artificial ultraviolet (UV) light in the early 20th century to facilitate the foundation of modern phototherapy. Today, a variety of coherent and noncoherent sources may be employed, from laser sources to non-laser sources (e.g., light-emitting diodes [LEDs]), as well as newer developments such as femtosecond lasers [31]. As photodynamic therapy, a minimally invasive and technically approved method, it was frequently applied in cancer treatment due to its successful nature of selectively destroying certain kinds of diseased tissues. The photodynamic therapy (PDT) procedure consists of three vital elements: visible light, photosensitizing agents (PS), and oxygen. Treatments start with the application of a photosensitizing drug, targeting the compound in tumor tissue. When there is sufficient material, the tissue is exposed to light at a wavelength that can be used in tissue (red light region; $\lambda > 600$ nm due to better penetration capabilities) [35, 36].

When the light turns on, energy from the activated photosensitizer transfers to oxygen molecules. This process generates singlet oxygen ($^1O_2$) and other reactive oxygen species (ROS). The harmful substances produced by light exposure lead to a cascade of chemical reactions that ultimately affect cell function and eventually lead to cell death. PDT mechanisms of action include direct cytotoxicity to cancer cells, tumor

vasculature compromise, initiation of anti-tumor immune responses, and local inflammatory reactions [37].

Initial trials demonstrated that light-sensitive chemicals could indeed kill bacterial cells. Accordingly, the modern era of photodynamic therapy (PDT) began with the recognition of hematoporphyrin derivatives and their selective tumor localization. More recent developments in photosensitizers, such as porphyrins and related compounds including phthalocyanines and chlorins, have enhanced strategies for deeper tissue penetration and improved the treatment efficiency of photodynamic therapy (PDT) [34].

The efficiency of photodynamic therapy (PDT) depends on several critical factors, including the quantum yield of singlet oxygen ($^1O_2$) production, the level of oxygenation in the target tumor tissue, and photosensitizer selectivity. Such lasers are usually used for photosensitizers with excitation in the range of 600-800 nm. In this way, they can perfectly permeate biological tissues and efficiently generate singlet oxygen ($^1O_2$). Furthermore, modern methods for photodynamic therapy (PDT) incorporate the efficiency of the photosensitizers, their stability, pharmacokinetic properties, and elimination from the body in a bid to enhance therapeutic outcomes and decrease side effects [37].

1.2.1 Mechanism of Action

The light sources employed in photodynamic therapy (PDT) are principally lasers, light-emitting diodes, and lamps. The choice of these sources is based on parameters including the exact target region, its absorption spectrum, and the required light dose. The toxic photosensitizing chemical at the photoactivated site becomes activated when subjected to sufficient light, allowing it to acquire and shuttle electrons. The oxygen molecules, in turn, accept electrons, slowly taking on one more before passing it to another. This results in the generation of cytotoxic reactive oxygen species (ROS) that can irreversibly damage microorganisms and target tissues by breaching the cell membrane and subsequently inducing cell death via necrosis or apoptosis. ROS encompasses not only free-radical molecules like superoxide ($O_2^{\bullet-}$), hydroperoxyl ($HO_2^{\bullet}$), hydroxyl ($^{\bullet}OH$), peroxy ($ROO^{\bullet}$), and alkoxy ($RO^{\bullet}$) radicals, but also non-radical reactive molecules such as hydrogen peroxide (H_2O_2) and singlet oxygen ($^1O_2$).

The ROS most frequently encountered are $O_2^{\bullet-}$, H_2O_2, and •OH. ROS is divided into two main families, the mechanisms of which are involved in photodynamic therapy (PDT). The first subtype is based on the formation of singlet oxygen ($^1O_2$) from photosensitizer (PS) molecules, which then interact with the substrate to form free radicals. The second type involves the uptake of energy from excited PS molecules, which subsequently transfer it to molecular oxygen, forming highly reactive singlet oxygen. The singlet oxygen can then react with lipids, proteins, and nucleic acids, inducing cell necrosis or apoptosis. Upon absorbing a photon, the photosensitizing agent is promoted to an excited state, which has three possible electronic states: an initial ground state (S0), a singlet excited state (Sn), and a long-lived triplet excited state. Upon absorption, several photo processes can occur, but the most likely deactivation path leads to relaxation to the lowest vibrational energy state. Fluorescence: This happens when a molecule in its ground energy state is excited to one of the lowest 2 states and then returns to where it initially was. The process leading to the lowest excited triplet state through a nonradiative mechanism is also called intersystem crossing and can followed by radiative decay through photon emission or trigger photochemical reactions [39].

In photodynamic therapy (PDT), substances (photosensitizers), when activated by photons, stimulate a triplet state, driving reactions of type I and type II. Type I reactions occur via an interaction between photosensitizers (PSs) and substrate molecules to produce free radicals. The primary mechanism by which stress occurs is through type I PDT reactions, which rely on the production of reactive oxygen species (ROS) through the generation of radicals and subsequent reactions mediated by O_2. The photosensitizer (PS) is delivered and specifically gathered in target cells, such as cancer cells. The photosensitizer absorbs light energy and transforms from its ground state to a singlet state after being exposed to certain wavelengths. Upon intersystem crossover, the excited state of the PS undergoes a conversion to a long-lived triplet state. The highly energized triplet state of the PS can directly interact with neighboring biomolecules such as lipids, proteins, and nucleic acids. During this process, there is a transfer of either an electron or a hydrogen atom, resulting in the formation of radical ions ($PS^{\bullet+}$ and $PS^{\bullet-}$). When a triplet PS interacts with a biomolecule, it can generate radicals that donate an electron to molecular oxygen (O_2), resulting in the formation of superoxide anions ($O_2^{\bullet-}$). Superoxide anions exhibit a relatively high level of stability,

although they can undergo further reactions to transform into more reactive molecules. Superoxide anions undergo mutagenesis, a process frequently facilitated by the enzyme superoxide dismutase (SOD), resulting in the formation of hydrogen peroxide (H_2O_2). This compound enables hydrogen peroxide to pass through the cell membrane and freely combine with other components inside. The Fenton reaction involves the reaction of hydrogen peroxide with metal ions, such as iron or copper. This reaction reduces the transition of metal ions by converting superoxide (OH•) into hydroxyl radicals (HO•). Hydroxyl radicals possess characteristics that render them extremely aggressive and capable of inflicting significant harm to biological components. Hydroxyl radicals initiate radical chain reactions by attacking other biological molecules, resulting in the formation of more radicals. The peroxyl radicals can cause further oxidative harm through a series of chain reactions, referred to as lipid peroxidation. This method exacerbates the cell's oxidative stress, leading to a chain reaction. The reactive oxygen species (ROS) produced from these reactions cause oxidative damage to essential biological components, including membranes, proteins, and DNA. Accumulated damage limits cellular function and ultimately causes cell death, either by apoptosis (programmed cell death) or necrosis (a form of cell destruction) [42]. In the presence of molecular oxygen, there is a limitation in the production of reactive oxygen species (ROS). Tumor cells are resistant to cell inactivation from photodynamic therapy (PDT) when exposed to low oxygen levels. Type II reactions rely on the occurrence of triplet-triplet annihilation. During these reactions, the photosensitizer (PS) in its excited triplet state has a reaction with oxygen in its triplet ground state. This results in the formation of singlet oxygen, which is highly reactive and cytotoxic. Both types of reactions occur simultaneously. The equilibrium between these two processes is contingent upon the specific photosensitizer (PS) used, as well as the concentrations of oxygen and substrate, and the affinity of the PS for the substrate. However, the creation pathway of singlet oxygen, specifically Type II reactions, is often regarded as the primary mechanism for PDT [40] (Figure 1.3).

Its course includes photon absorption, which induces photoactivatable molecules (PSs) to transit from the ground state to an excited state. Concerning the ground state electron moving to higher energy orbital and 1st excited singlet state(S), since this is inherently unstable, it can relax and is lost either as light emission or internal conversion. This

excited state is equilibrium and can be easily relaxed to the ground state by light emission (fluorescence) or resonate energy transfer. The second thing that happens is called an intersystem crossing, intersystem crossing, where S1 - the excited singlet state that was previously mentioned - falls to another, more stable (and likely longer-lived) excited triplet state (T1). The triplet state possesses unpaired, parallel electrons and thus is longer lived than the singlet state. A long triplet-state lifetime is important because it allows for photochemical interactions to take place. O2 Triplet species excited by PS interact with ground triplet O2. Photo-induced conversion of ground-state molecular oxygen to singlet oxygen (^{1}O2). a powerful form of oxygen that reacts poorly with PS through energy transfer. Such light-dependent ROS of lipid peroxidation and protein oxidation type can lead to oxidative damage to the basic components of plant cells [41,42].

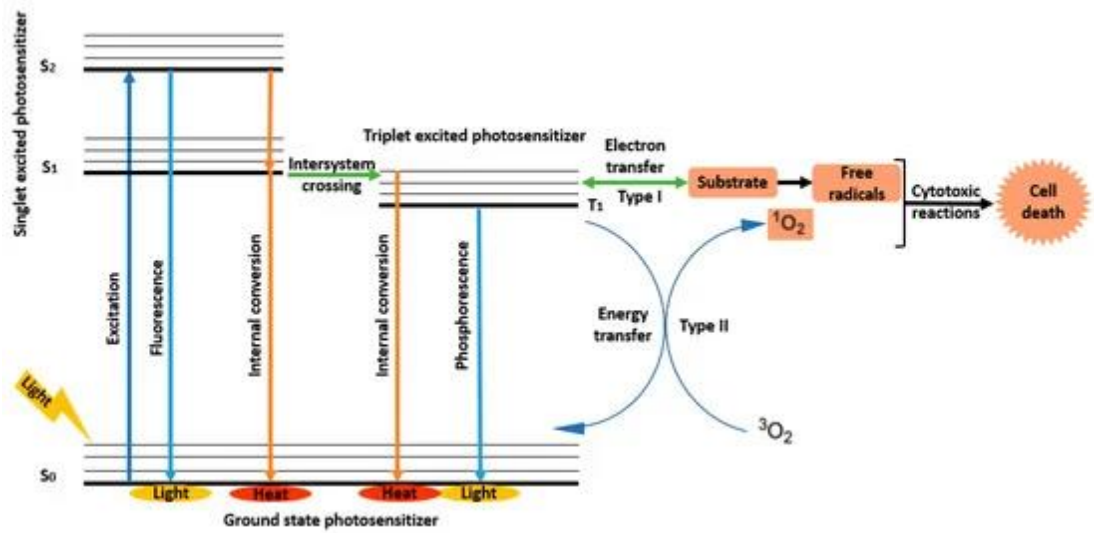

Figure 1.3: Depiction of the mechanism of photodynamic therapy (PDT) [38].

1.2.2 Photosensitizers

Photosensitizing agents (PSs) are required for photodynamic therapy (PDT) that absorb light to generate reactive oxygen species (ROS) through photochemical reactions. In the dark, these agents are non-toxic, which allows PDT to selectively kill cancer cells with minimal damage to normal tissue. PSs are divided mainly into three generations: first-generation PSs including hematoporphyrin derivative (HpD) and porphyrin, second-generation PSs including chlorins, porphyrin derivatives such as chlorin e6 and verteporfin, methylene blue, toluidine blue, phthalocyanines,

indocyanine green (ICG), and aminolevulinic acid (ALA), and third-generation PSs which have been developed for specific accumulation at tumor sites [43].

The modern renaissance in PDT stemmed from the work of Lippin and Schwartz at the Mayo Clinic detection and characterization of hematoporphyrin derivative (HpD) first reported in 1960 with major impetus provided by pioneering publications in both basic science and clinical application. A purified form of HpD, now commercially available as Photofrin, was developed in 1983. The PS Photofrin was the first PS to gain regulatory approval (in over 40 countries throughout the world, including the US for the treatment of certain types of cancer) [44].

Despite success in treating various cancers with first-generation agents such as PS Photofrin, there are several limitations: suboptimal tumor selectivity, inadequate light absorption, and poor light penetration into some tumors owing to a relatively short wavelength absorption (630 nm), prolonged patient skin photosensitivity, and uncertainties regarding the complex nature of structure mixture. In response to these limitations and goals of refining treatment, numerous tactics have been explored for the development of selective agents that are less likely to produce side effects, specifically skin phototoxicity. New generation PSs (second generation) such as tiraporide, P2, and hypericin have been developed in recent years, and introduced in clinical trials. The majority of these are cyclic tetrapyrroles, including substituted porphyrin, chlorin, and bacteriochlorin derivate species. Some of them are Tookad, Antrin, benzoporphyrin derivative monocarboxylic acid (BPD-MA), Purlytin, Foscan, and zinc (II) phthalocyanine (Pc) with high absorption in the wavelength range 650-750 nm [45].

Ideal PSs would be chemically pure, of known specific composition, in stable forms at room temperature, and prepared via facile synthesis. They should be minimally dark toxic, have target tissue accumulation and rapid washout from normal body tissues, cause low systemic toxicity to normal tissue, have high absorption and a large molar absorbance coefficient or extinction coefficient (ε) in the range of longer wavelengths (red-NIR), exhibit excellent photochemical reactivity, be non-expensive and commercially available, easy to prepare and soluble in biological fluid [46].

Subsequently, a chlorin derivative (chlorin a and chlorin b) that occurs naturally has been developed to enhance PDT. chlorin a is not applicable in PDT, it forms highly ordered aggregates, and its solubility in physiological fluids is low, however may be used as a good starting material for designing new PS that fits with pharmaceutical demands [44].

1.2.3 Light Sources Used in PDT

Photodynamic therapy (PDT) is a treatment that uses light to interact with tissue and activate the Proliferative Response (PS). The interaction between light and tissue is based on the optical qualities, size, shape, and density characteristics of the biological tissue. Tissues consist of cells and components of different sizes, ranging from nanometers to micrometers. The optical properties of tissues can vary based on the kind of tissue and may exhibit inhomogeneity. The absorption and scattering characteristics of key components of tissues, such as hemoglobin, water, fat, and ela, directly impact the absorption and scattering processes inside the tissues. The absorption coefficient of collagen and melanin is generally high; however, it is usually concentrated in certain locations with low concentrations. Water is the primary factor for λ (wavelength) more than 1000 nm, with its influence varying depending on the kind of tissue. The therapeutic window for photodynamic therapy (PDT) is determined by the optical characteristics and concentration of tissue constituents, as well as the photosensitizer (PS) and its concentration. This window is specified inside the optical window. The typical therapeutic range is often limited to approximately 600-950 nm, as water absorption becomes more pronounced and could lead to an excessive therapeutic range [51].

Accurate light supply at an optimum dose is essential for the clinical success of Photodynamic Therapy (PDT) as it relies on illumination. Technological advancements have facilitated the administration of light to a significant portion of the human body, rendering it suitable for treating a range of disorders. The selection of a radiation source is contingent upon the tumor's specific position and depth. However, accurately estimating dosimetry is a challenge. The most feasible approach is to use lower irradiation energies for longer photodynamic treatments [50].

Red laser light at 650 nm is chosen for Photodynamic Therapy (PDT) due to its optimal balance between tissue penetration and photosensitizer activation. This wavelength falls within the "therapeutic window" where biological tissues exhibit low absorption and scattering, allowing deeper light penetration. Chlorin e6, a second-generation photosensitizer derived from chlorophyll, is preferred due to its high absorption coefficient, efficient ROS production, and favorable pharmacokinetic properties. Ce6 accumulates preferentially in cancer cells [52].

1.3 Electrochemical Sensors

Electrochemical sensors, particularly those integrated with biosensing capabilities, represent a significant advancement in the field of chemical analysis due to their low cost, high detection efficiency, and versatility. These sensors utilize electrochemical transducers to detect and quantify various substances, leveraging the specific recognition abilities of biological elements like enzymes and antibodies [53].

Electrochemical sensors are vital tools in modern chemical analysis, combining biological recognition elements with electrochemical transducers to detect and quantify diverse substances. The integration of biosensors with chemical sensors approximately fifty years ago allowed for the utilization of the specific recognition abilities of biological components, such as enzymes and antibodies [54].

Electrochemistry, a field of study that began with the research of Volta, Galvani, Davy, and Faraday, experienced a period of silence until the early 20th century when M. Cremer invented the glass electrode and J. Heyrovsky discovered polarography. This marked the birth of modern electrochemistry, leading to the development of well-known methods and electrode types. Electrochemical methods like potentiometry, Volt amperometry, and conductimetry have experienced significant development due to their high sensitivity [55].

Chemical sensors are devices that convert chemical information from an analyte's chemical reaction or physical properties into analytically useful signals. They consist of a chemical recognition system called a receptor, which converts the information into a measurable form of energy, and a physicochemical transducer that converts the energy into a useful analytical signal. Modern sensor systems typically include a

sample delivery unit and a data processor. The receptor part of chemical sensors is based on three basic principles of stimulus: physical, chemical, and biochemical. The main function of the receptor is to provide the sensor with a high degree of selectivity for the analyte to be measured. Some sensors are class-specific, such as sensors or biosensors for phenolic compounds or whole-cell biosensors for biological oxygen demand. The transducer transfers the signal from the recognition system's output domain into an output signal, usually electric, amplified by electronics, and converted into useful data [56].

The main types of electrochemical sensors include amperometric, potentiometric, voltammetric, and electrophotonic sensors. Each type has unique operating principles and applications, ranging from health monitoring devices like glucose sensors to environmental sensors for detecting pollutants. The development and refinement of these sensors involve overcoming challenges related to selectivity, sensitivity, and anti-fouling. Moreover, the choice of electrode materials and configurations, such as enzyme-modified electrodes or DNA aptamer-based sensors, significantly influences the performance and applicability of these sensors. Two-electrode (2E) and three-electrode (3E) systems are common configurations in electrochemical methods, offering distinct advantages and limitations. The two-electrode system consists of a working electrode and a counter electrode, used in situations where the potential difference between the two electrodes is of primary interest. It is commonly used in battery and fuel cell research, where large currents are involved, and suitable for applications where precise control over the working electrode potential is not critical.

The three-electrode system adds a reference electrode, significantly improving the control and measurement precision of the working electrode potential. It is essential for most analytical electrochemical techniques and is ideal for cyclic voltammetry, chronoamperometry, and other techniques that require precise potential control. Applications include analytical chemistry for studying redox reactions and mechanisms, electrodeposition, corrosion studies, and electroplating processes where control over electrode potentials is crucial [57] (Figure 1.4).

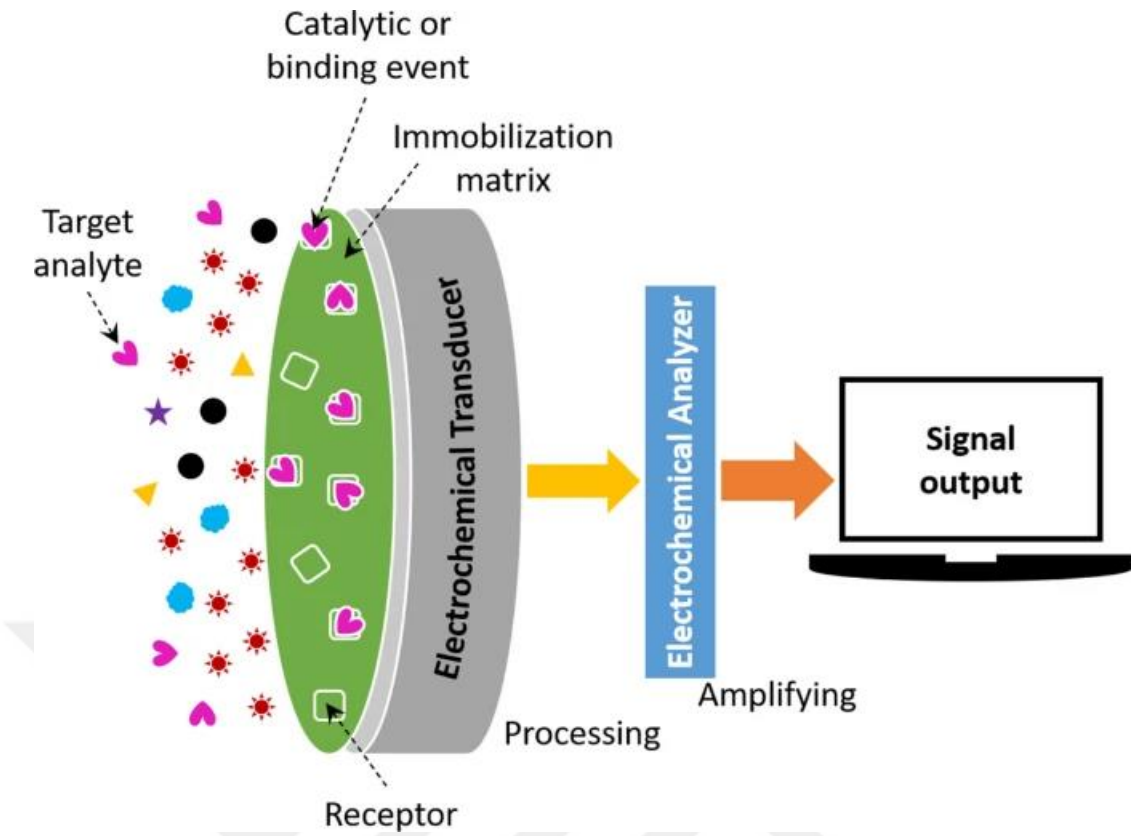

Figure 1.4: The configuration and working principle of an electrochemical sensor. The target analyte in a sample is recognized by the receptors fixed on the electrode surface, resulting in a catalytic or binding event. The signal output is generated from the translation of the physicochemical changes due to target–receptor interactions, which can be displayed in the different electrochemical data depending on the types of measurement [58].

1.3.1 Screen-printed electrodes

Screen-printed electrodes (SPEs) represent a significant advancement in the field of electrochemical sensing and biosensing. These electrodes are fabricated using a screen-printing technique, which allows for the mass production of electrochemical sensors with high reproducibility and low cost. The versatility and accessibility of SPEs have revolutionized the design and application of sensors in various fields, including environmental monitoring, medical diagnostics, food safety, and industrial process control. SPEs represent a significant advancement in the field of electrochemistry, bringing decades of miniaturization and innovation to practical applications. They serve as a cost-effective, disposable, and highly reproducible

alternative to the traditional setup involving separate solid electrodes and a glass volumetric cell. SPEs are created by depositing various ink layers onto a flat substrate, forming a compact device that integrates the working, counter, and reference electrodes. The fabrication of SPEs leverages industrial-scale manufacturing methods such as screen-printing, roll-to-roll, and pad-printing. These techniques provide versatility and precision, allowing for the deposition of conductive inks onto substrates with great accuracy. This approach replaces older, less reproducible methods like drop-casting and dip-coating, streamlining the production process and enhancing the quality of the electrodes [59]. Screen-printed electrodes are widely used in academic literature and have transitioned into commercial products due to their wide range of advantageous properties and low cost compared to commercial external electrodes. These advantages include the combination of all three electrodes on one device, minimization of the electrochemical platform, the flexibility of electrode shape and size, a wide range of electrode materials, a wide array of printable substrates, mass production capabilities, high reproducibility, sensitivity, and accuracy, and ability to bulk-modify inks for bespoke production. screen-printed electrodes offer an economical, reproducible, disposable, and robust platform as an alternative to traditional electrochemistry setups. They offer numerous advantages, including cost-effectiveness, flexibility, and the ability to bulk-modify inks for bespoke production. However, there are drawbacks to SPEs, such as batch-to-batch variation and poor benchmarking standards [59, 61] (Figure 1.5).

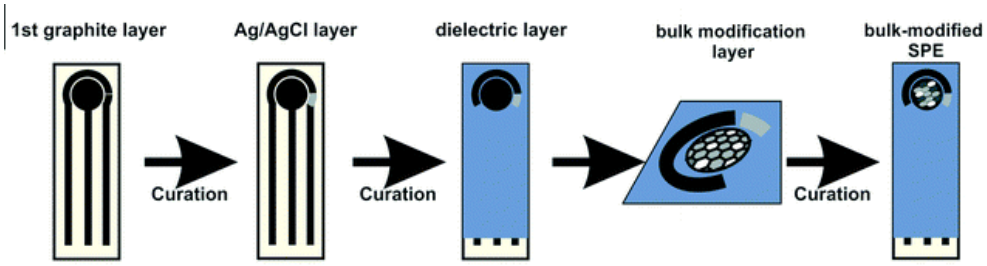

Figure 1.5: Overall scheme of screen-printing [59].

1.3.2 ROS detection via SPE

Reactive oxygen species (ROS) play a crucial role in various biological mechanisms, including apoptosis, necrosis, autophagy, vascular occlusion, and antitumor immune responses. Apoptosis is a process where cells undergo controlled destruction to remove

damaged or unnecessary cells. ROS induces apoptosis through various pathways, such as the mitochondrial pathway, death receptor pathway, and endoplasmic reticulum stress. Necrosis is a form of cell death characterized by the uncontrolled release of cellular contents, leading to inflammation and damage to surrounding tissues. ROS contributes to necrosis through oxidative damage, ATP depletion, and lipid peroxidation [39]. ROS detection faces limitations due to the unique properties of different ROS, such as lifetime, diffusion rate, and generation sources, which can lead to inaccurate measurements. Low and unstable concentrations at these sources can make techniques inappropriate for ROS detection, especially in living cells. Researchers have developed techniques like ESR, MS, spectrophotometry, HPLC, fluorescence spectroscopy, and electrochemical methods. However, most methods are qualitative or semi-quantitative, which can be poorly selective and sensitive due to autofluorescing substances in cells [62]. Carbon-based electrodes have gained significant interest in the field of ROS detection due to their distinctive characteristics in recent years. Graphene, carbon nanotubes, and carbon nanofibers electrodes offer a large surface area along with excellent electrical conductivity, chemical stability, and biocompatibility. Carbon-based electrodes possess specific attributes that make them very suitable for electrochemical sensing applications. Furthermore, the surface of carbon materials can be easily modified through functionalization to customize their redox potentials, resulting in enhanced sensitivity and selectivity towards specific reactive oxygen species (ROS).

An effective method for improving the efficiency of carbon-based electrodes in detecting reactive oxygen species (ROS) involves the incorporation of redox mediators, such as hydroquinone. hydroquinone’s primary role is to serve as an electron carrier, facilitating the movement of electrons between the surface electrode and ROS in a given sample. Therefore, this mediation improves the sensitivity and lowers the limits of detection for electrochemical signals.

Hydroquinone (HQ), a phenolic compound, has unique electrochemical properties due to its reversible exchange of electrons and protons. When exposed to light, HQ can be oxidized to benzoquinone (BQ) through a photogenerated singlet oxygen reaction. This redox transformation generates a photocurrent proportional to the concentration of hydroquinone in the solution, making it useful for various analytical applications.

Quinones, including benzoquinones, naphthoquinones, and anthraquinones, have significant clinical applications, particularly in cancer treatment. Quinones are effective generators of singlet oxygen and reactive oxygen species (ROS), which play a critical role in physiological and pathological processes. The interaction of hydroquinone and its redox reactions under laser application is a vital area of study, offering insights into its analytical uses and the broader implications of quinone-induced ROS in biological systems [64, 66] (Figure 1.6).

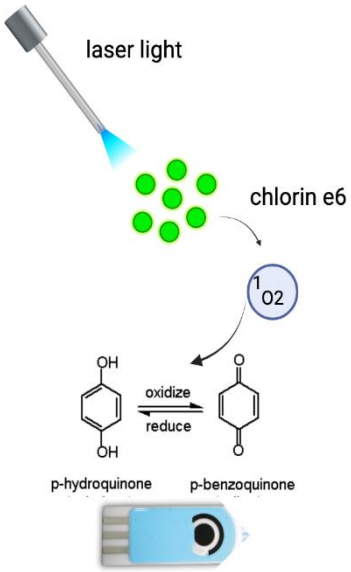

Figure 1.6: Illustration for the produced singlet oxygen ($^1O2$) and redox transformation of hydroquinone (Drawn in BioRender)

In this master thesis, the aim was to advance the understanding and application of carbon-based electrodes in biomedical engineering, particularly focusing on their role in detecting reactive oxygen species (ROS) with enhanced sensitivity and specificity. The research explored novel methodologies, including the utilization of hydroquinone as a redox mediator, to optimize the detection capabilities of screen-printed electrodes (SPEs) in the context of photodynamic therapy (PDT) and other biomedical applications.

Chapter 2

Materials and Methods

This study has two primary experimental sets focused on improving the effectiveness of photodynamic therapy (PDT) for the treatment of ovarian cancer through the application of photodynamic and sensor-based detection techniques. In the initial phase, a 655-nm red diode laser light is utilized to treat SKOV-3 human ovarian cancer cells by photodynamic therapy. Subsequently, the cells are incubated with Chlorin e6 (Ce6) as the photosensitizer. Afterward, the cells are exposed to the same 655-nm red diode laser light to induce photodynamic activity. The duration of Ce6 incubation was 1 hour. The second primary set incorporates a novel sensor-based methodology in conjunction with PDT. SKOV-3 cells were grown and exposed to various concentrations of Ce6, after that hydroquinone (HQ) solution was added. The SKOV-3 cells and HQ are used together on the surface of a screen-printed electrode (SPE). Photodynamic therapy is performed inside a Faraday cage to reduce external electrical interference, and signal capture is done using chronoamperometry. After doing these experimental configurations, a range of analyses are carried out to evaluate the effectiveness of the therapy and the reactions of the cells. The analyses encompass cell viability assessment using the MTT assay, detection of intracellular reactive oxygen species (ROS) production, and monitoring of sensor-based signals during photodynamic therapy (PDT) applications. The results offer valuable information regarding the internalization of photosensitizers by cells, the production of reactive oxygen species (ROS), and the overall efficacy of photodynamic therapy (PDT) in treating ovarian cancer cells. Essentially, the materials and methods portion of this paper provides a thorough description of the methodologies and experimental settings employed to improve the effectiveness of photodynamic therapy (PDT) and include sensor-based detection approaches in cancer treatment.

2.1 Cell Culture

SKOV-3 human ovarian cancer cells were utilized in this study. The SKOV-3 cells were grown in 75 cm^2 tissue culture flasks in McCoy's 5A cell culture medium, which included 1% L-Glutamine, 1% Penicillin-Streptomycin, and 10% fetal bovine serum (FBS), maintained at 37°C in a humidified atmosphere containing 5% CO_2. The cells were incubated until they reached 80% confluency or higher. Upon reaching the desired confluency, the cells were detached from the flask surface using Trypsin-EDTA (10X diluted to 1X with Phosphate Buffered Saline, PBS) after washing with PBS. Following detachment, $2x10^4$ cells per well were seeded into a 96-well plate for subsequent experiments.

2.2 Photosensitizers

Chlorin e6 (Ce6) (Figure 2.1) is a photosensitizer that belongs to the second generation and is generated from chlorophyll a. It has a tetrapyrrole ring structure that is similar to porphyrins featuring a central magnesium ion. However, this magnesium ion is frequently eliminated during the synthesis process, leading to the formation of a chlorin structure without magnesium. (67) Ce6 demonstrates a strong capacity to generate reactive oxygen species and possesses powerful anticancer properties, which makes it a suitable candidate for photodynamic treatment (PDT). The central framework comprises a tetrapyrrole ring system, identical to heme and chlorophyll, accompanied by several functional groups that augment its photochemical characteristics. The photosensitizer Chlorin e6 (Ce6) was employed in this study. Stock solutions of Ce6 were initially prepared using DMSO and then diluted with McCoy's 5A cell culture medium to achieve final concentrations of 5, 10, 25, 50, and 100 μM, freshly prepared before each experiment.

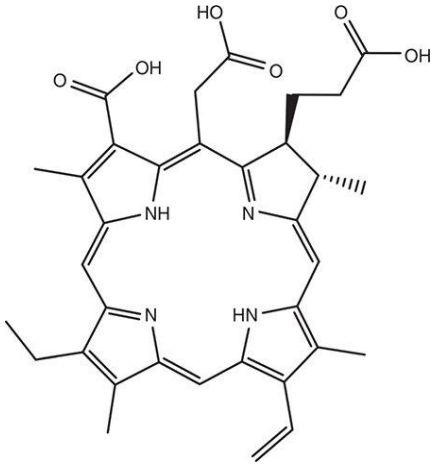

Figure 2.1: Structure of Chlorin e6 [66].

2.3 Light Sources

A 655-nm diode laser (Figure 2.2) was used as the light source for the experiments. The red 655-nm diode laser provided continuous radiation through optical fiber. The laser devices were positioned using various optomechanical equipment to irradiate samples at a constant distance of 7 cm from the tip of the optical fiber to the optical plate. The output power of the 655-nm diode laser was set to 0.5 W and measured with a digital power meter (Thorlabs, Newton, NJ, USA) before each experiment. The required application time to achieve a specific energy density was calculated using the following equation (2.1):

Equation (2.1): Energy Density (J/cm²)=Area (cm²)Power (W)×Time (s)

To obtain an energy density of 25 J/cm², the 655 nm laser light was applied for 195 seconds.

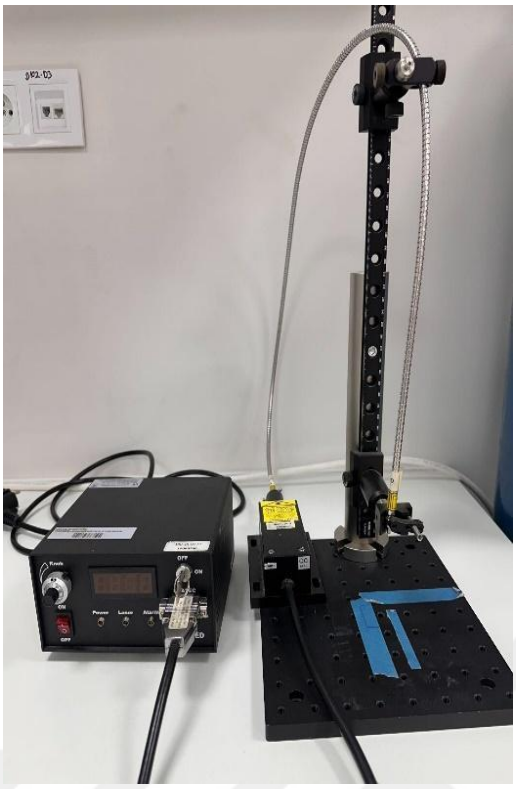

Figure 2.2: 655-nm Diode Laser Device

2.4 Anticancer PDT Applications

The experiments included the following groups:

- Control Group: Neither photosensitizer (PS) addition nor light application.
- PS Group: Incubation with PS only.
- Laser Group: Irradiation with 655 nm light at 25 J/cm² energy density.
- Only PDT Group: Irradiation with PDT laser light after specific incubation times with the PS.

For the Only PDT Group, SKOV-3 cells were incubated for 24 hours at 37°C in a 5% CO_2 humidified atmosphere to allow adherence to the 96-well plate surfaces. Subsequently, McCoy's 5A cell culture medium was removed, various concentrations of the PS solution were added, and cells were incubated with the PS for 1 hour at 37°C in a 5% CO_2 humidified atmosphere. After incubation, PS solutions were removed,

cells were washed once with PBS to remove excess PS, fresh cell culture medium was added, and cells were irradiated with 655-nm diode laser light at 0.5 W for PDT action.

In the PS Group, different concentrations of PS solutions were added after removing the cell culture medium, and cells were incubated various times at 37°C in a 5% CO_2 humidified atmosphere. After incubation, PS solutions were removed, cells were washed once with PBS, a fresh cell culture medium was added, and cells were irradiated with 655-nm diode laser light at 0.5 W output. Finally, cells were incubated with a cell culture medium at 37°C in a 5% CO_2 humidified atmosphere to match the control group conditions. After completing the applications for each group, necessary analyses were performed (Figure 2.3).

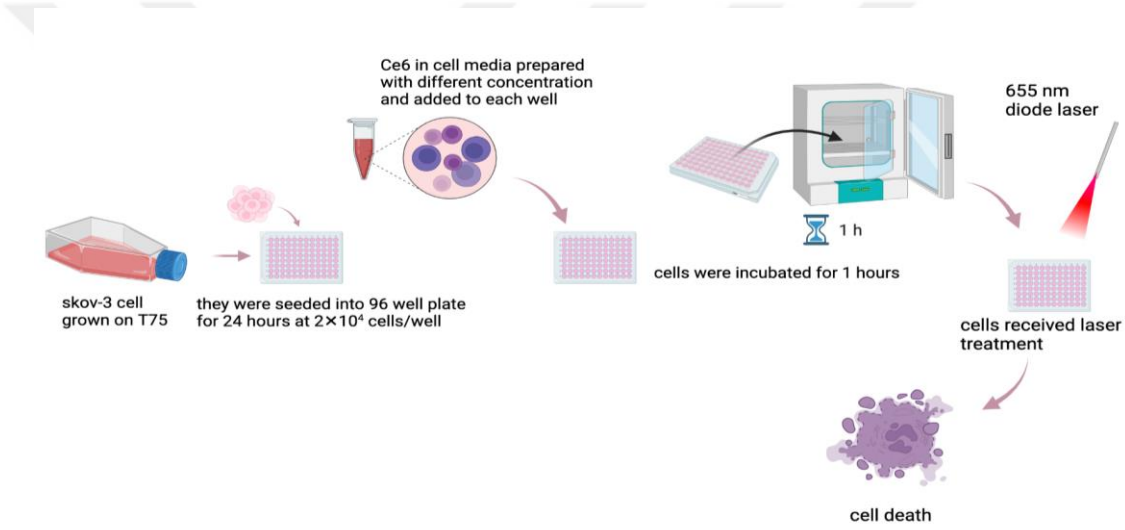

Figure 2.3: Illustration for the PDT Experimental Setup (Drawn in BioRender)

2.5 Cell Viability Analysis

The MTT cell viability assay was employed to determine cellular viability. The assay uses 3-(4,5-dimethylthiazol-2-yl)-2,5-diphenyl tetrazolium bromide (MTT), a colorimetric assay that indicates cellular viability through a color change. MTT, which is yellowish due to its tetrazole structure, is converted to purple formazan crystals by the succinate dehydrogenase enzyme in the electron transport chain of the inner mitochondrial membrane during metabolic activity. The absorbance of purple formazan crystals was measured spectrophotometrically, providing cell viability data.

The MTT assay was conducted for all experimental groups. A 5 mg/mL MTT stock solution was prepared in distilled water and diluted to a 10% MTT solution with serum-free McCoy's 5A cell culture medium. After completing the experiments, the cell culture medium was removed from SKOV-3 cells, and 100 µL of 10% MTT solution was added to each well of the 96-well plate. Cells were incubated for 2 hours at 37°C in a 5% CO_2 humidified atmosphere. After incubation, the MTT solution was removed, and 100 µL of dimethyl sulfoxide (DMSO) was added to each well to dissolve the formazan crystals. The absorbance was measured using a multi-plate microplate reader (Synergy™ HTX Multi-Mode Microplate Reader, BioTek, Winooski, USA) at 570 nm. All steps of the MTT analysis were performed in the dark to prevent MTT deterioration.

2.6 Intracellular Reactive Oxygen Species Production Analysis

Intracellular ROS production was assessed after Ce6-mediated PDT applications using the ROS-sensitive probe 2′,7′-Dichlorofluorescein diacetate (DCFH-DA) (Sigma Aldrich, St. Louis, MO, USA). DCFH-DA is a lipophilic, non-fluorescent compound that passes through cell membranes via passive diffusion and is deacetylated to 2′,7′-Dichlorofluorescein (DCFH) inside the cells. DCFH is then oxidized to the highly fluorescent compound DCF in the presence of ROS, with fluorescence intensity directly correlating with ROS levels.

A 40 mM DCFH-DA stock solution was prepared in DMSO and diluted to 0.1 mM with McCoy's 5A cell culture medium containing 1% FBS. The cell medium was removed 24 hours after seeding, and 0.1 mM DCFH-DA solution was added to the cells, followed by 45 minutes of incubation at 37°C in a 5% CO_2 humidified atmosphere in the dark. After incubation, the DCFH-DA solution was removed, cells were washed once with PBS to eliminate excess DCFH-DA, fresh cell culture medium was added, and the experimental protocol was applied. Upon completion, the fluorescence intensity of DCF was measured using a multi-plate reader with excitation at 485/20 nm and emission at 528/20 nm.

2.7 Reactive Oxygen Species Generation Capacity of Chlorin e6

The ability of Chlorin e6 (Ce6) to produce singlet oxygen was evaluated using 1,3-diphenylisobenzofuran (DPBF). DPBF is a chemical compound that undergoes a reaction with singlet oxygen to produce 1,2-dibenzoylbenzene, leading to a reduction in absorbance at 415 nm. The study involved the preparation of Ce6 solutions in dimethyl sulfoxide (DMSO) and the addition of a fresh DPBF solution. 8 mM (4uL) DPBF was added to chlorin e6 at concentrations of 10, 25, 50 and 100 μM. The initial absorbance spectrum of the Ce6 and DPBF mixture was recorded at 415 nm. A 655 nm diode laser was applied to the samples, and the absorbance spectrum was measured at 415 nm. The decrease in absorbance at 415 nm before and after laser irradiation was calculated, and it was directly proportional to the amount of singlet oxygen produced.

The experiment involved varying laser power levels with 100 μM Ce6 solutions, applied for 30 seconds each time. Laser power levels were set to 100, 200, 300, and 400 mW, with each power setting applied for 30 seconds. Absorbance measurements at 415 nm were taken before and after irradiation to determine the relationship between laser power and singlet oxygen production.

2.8 Electrochemical Sensor Analysis to Determine the Reactive Oxygen Species Generation Capacity of Chlorin e6

This experiment studies the application of an electrochemical sensor to quantify the formation of reactive oxygen species (ROS) in solutions containing Ce6 and HQ. The stock solutions were made by dissolving Ce6 in phosphate-buffered saline (PBS) and combining it with a mixture of Ce6 stock solution and HQ stock solution. screen-printing Electrode (SPE) was utilized for electrochemical experiments. A volume of 100 μL of the Ce6-HQ combination was deposited onto the surface of the electrode.

Chronoamperometric measurements were conducted both before and following the laser application. Before the laser application, the baseline signal was captured at a

voltage of 0 V for 75 seconds. The laser device was configured to emit a power of 500 mW with an energy density of 25 J/cm². The samples were exposed to the laser for 3 minutes and 15 seconds. The formation of reactive oxygen species (ROS) was continuously monitored in real-time during and after each laser treatment. Also, to understand the effect of laser power, 100 µM of Ce6 solution was mixed with HQ and added to the surface of the screen-printed electrode (SPE) in a droplet form. Baseline sensor signals were recorded for 70 seconds before laser irradiation. The experiment was repeated with a 100 µM Ce6 solution while varying the laser power at 100, 200, 300, and 400 mW, each applied for 30 seconds. Real-time sensor signals were recorded during each laser power setting (Figure 2.4).

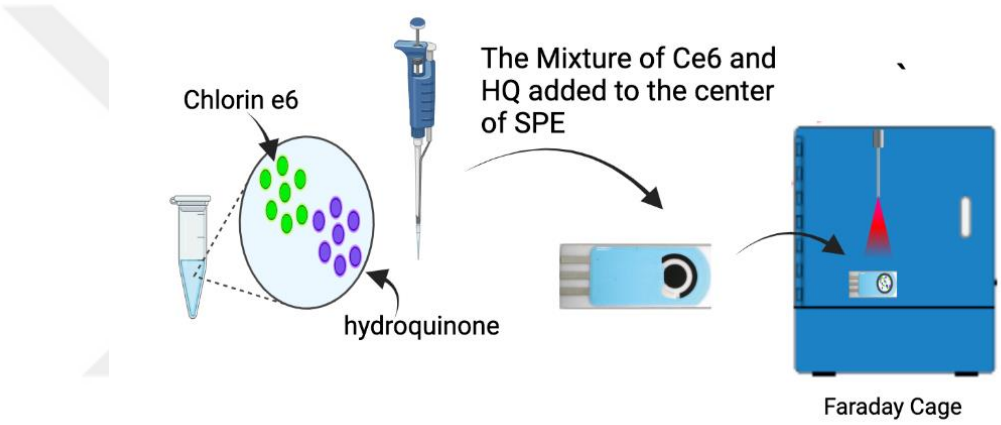

Figure 2.4: Illustration for the Electrochemical Sensor Experimental Setup (Drawn in BioRender)

2.9 Electrochemical Sensor Analysis to Determine the Intracellular Reactive Oxygen Species Production

The electrochemical sensor experiments were designed to evaluate the photodynamic effect on SKOV-3 cells in the presence of Chlorin e6 (Ce6) and hydroquinone (HQ). SKOV-3 ovarian cancer cells were cultured in a 96-well plate overnight at 37°C in a 5% CO_2 humidified atmosphere to allow for cell adherence. Different concentrations of Ce6 were added to each well and incubated for 1 hour. Following incubation, Ce6 was removed, and the cells were washed twice with phosphate-buffered saline (PBS) to eliminate any unabsorbed Ce6. A 5 mM HQ solution was prepared fresh before the

experiment. Subsequently, 100 µL of the HQ solution was added to each well containing the SKOV-3 cells. Using a single-channel pipette, 100 µL of the cell suspension from each well was carefully aspirated, ensuring no air bubbles were introduced. The cell suspension (SKOV-3 cells and HQ solution) was transferred to Eppendorf tubes. This mixture was then applied onto the surface of Screen-Printed Electrodes (SPEs) as a droplet. The laser device was positioned inside a Faraday cage, which was then sealed to ensure proper insulation. The distance and parameters of the laser setup were maintained identical to those used in the photodynamic therapy (PDT) experiments. Chronoamperometry was employed to record signals, with a potential of -0.05 V applied to the SPE.

Initial signals were recorded for 70 seconds before laser application. The 655-nm diode laser, with parameters identical to those used in the PDT setup, was applied to the SPE surface containing the SKOV-3 cells and HQ solution. Signals were continuously recorded during the 195 seconds of laser application, capturing real-time electrochemical changes. The recorded electrochemical signals were analyzed to determine the effects of PDT on SKOV-3 cells in the presence of HQ. Comparative analysis was performed between pre- and post-laser application signals to evaluate the impact of the PDT process.

By adhering to these detailed procedures, the study aimed to assess the efficacy of PDT in conjunction with Ce6 and HQ on SKOV-3 cells, using an electrochemical sensor to monitor real-time changes. This setup ensured controlled conditions and accurate measurements, contributing valuable data toward understanding the photodynamic effects on cancer cells (Figure 2.5).

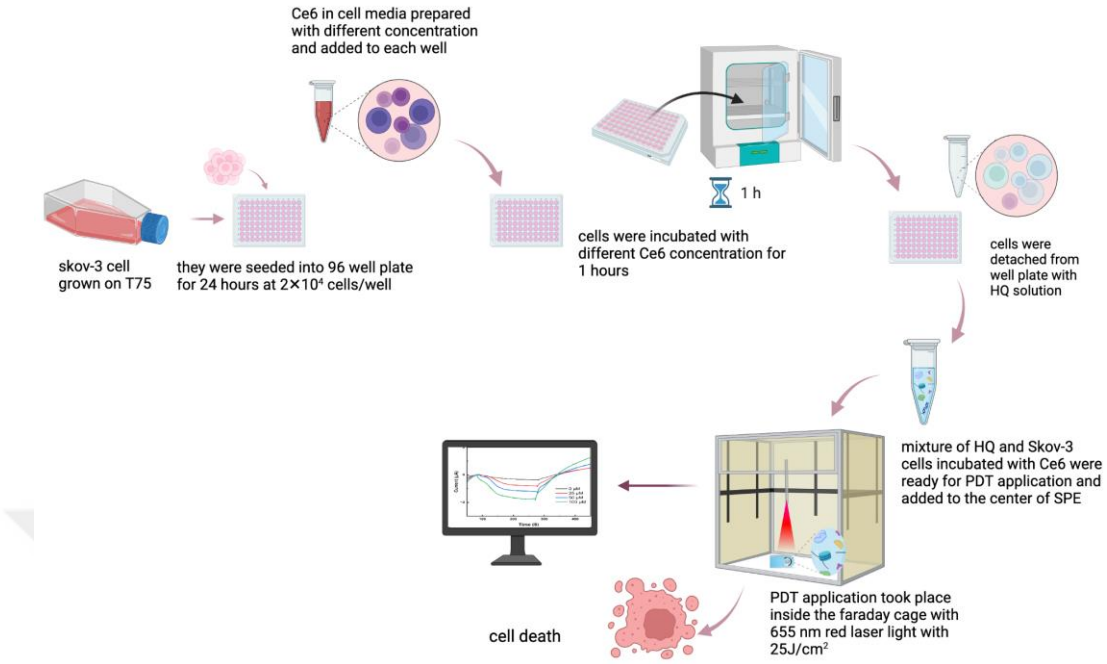

Figure 2.5: Illustration for the Electrochemical Sensor Analysis to Determine the Intracellular Reactive Oxygen Species Production Experimental Setup (Drawn in BioRender)

2.10 Statistical Analysis

Statistical analysis was carried out using Origin OriginPro 2024 and GraphPad Prism Version 9.5.1 (GraphPad Software Inc., La Jolla, CA, USA) software to ensure robust and reliable results. Descriptive statistics, including mean, standard deviation, and percentage change, were calculated to summarize the experimental data. For normally distributed data, parametric tests such as one-way ANOVA followed by post hoc Tukey's test were applied to compare multiple groups. Statistical significance was set to $p < 0.05$. All experimental data were presented as mean ± standard deviation (SD), and graphical representations of the results were created using GraphPad Prism to visualize trends and differences effectively. These rigorous statistical methods ensured the accuracy and reproducibility of the findings, highlighting the significance of the effects observed in the study.

Chapter 3

Results

3.1 Effect of Laser Light on Skov-3 Cells

The effect of laser light on the viability of Skov-3 cells was evaluated by determining the proportion of living cells following exposure to photodynamic therapy (PDT) energy density of 25 J/cm². The vitality of the cells was compared between the control cells that were not treated and the cells that were treated with laser light at the prescribed energy density. (Figure 3.1) demonstrates that the cell viability of the untreated control group (0 J/cm²) was adjusted to 100%, acting as an indicator for comparison. The cells that were subjected to 25 J/cm² of laser light showed a cell viability of around 10.85% increase, which was comparable to that of the control group. These findings indicate that exposing Skov-3 cells to laser light with an energy density of 25 J/cm² does not have a major impact on their viability. The absence of a substantial reduction in cell viability suggests that the tested PDT regimen does not exhibit toxicity towards Skov-3 cells under the given conditions.

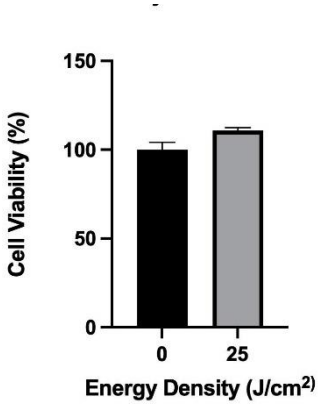

Figure 3.1: Cell viability analysis after laser irradiation Each bar represented the average of the normalized with respect to the control group.

3.2 Cytotoxicity of Photosensitizers on Skov-3 Cells

The effect of the photosensitizer Ce6 on Skov-3 cells has been evaluated by measuring their viability after performing photodynamic treatment (PDT) with an energy density of 25 J/cm². Cell viability was evaluated at various concentrations of Ce6 (0, 10, 25, 50, and 100 µg/ml), and the outcomes were compared between cells that were not treated (0 J/cm²) and cells that were subjected to laser light (25 J/cm²). Figure 3.2 shows that cell viability remained consistently high, close to 100%, across all concentrations of Ce6 in the absence of PDT (0 J/cm²). This indicates that Ce6 alone did not have a substantial harmful effect on Skov-3 cells. Nevertheless, when subjected to PDT at 25 J/cm², a significant reduction in cell viability was noticed as the concentration of Ce6 increased. More precisely, the viability of cells decreased dramatically when exposed to concentrations of 25, 50, and 100 µg/ml of Ce6. The viability percentages reduced to around 49% in 25µg/ml Ce6 concentration and this number reached 91.1%, and 91.6% for 50 and 100 µg/ml respectively.

The statistical analysis demonstrated that the decreases in cell viability were extremely substantial (****, $p < 0.0001$) in comparison with the control groups that were not treated. The results demonstrate a strong and harmful effect of Ce6-mediated PDT on Skov-3 cells, especially when larger concentrations of Ce6 are used. The results indicate that the use of Ce6 and PDT in combination significantly decreases the viability of Skov-3 cells in a manner that is dependent on the concentration. The substantial reduction in cell viability seen at higher concentrations of Ce6 suggests that Ce6-mediated PDT holds great promise as a therapeutic strategy for specifically targeting Skov-3 cells. Subsequent investigations could prioritize the optimization of the photosensitizer concentration and parameters of photodynamic therapy (PDT) to enhance therapeutic effectiveness while limiting potential adverse reactions.

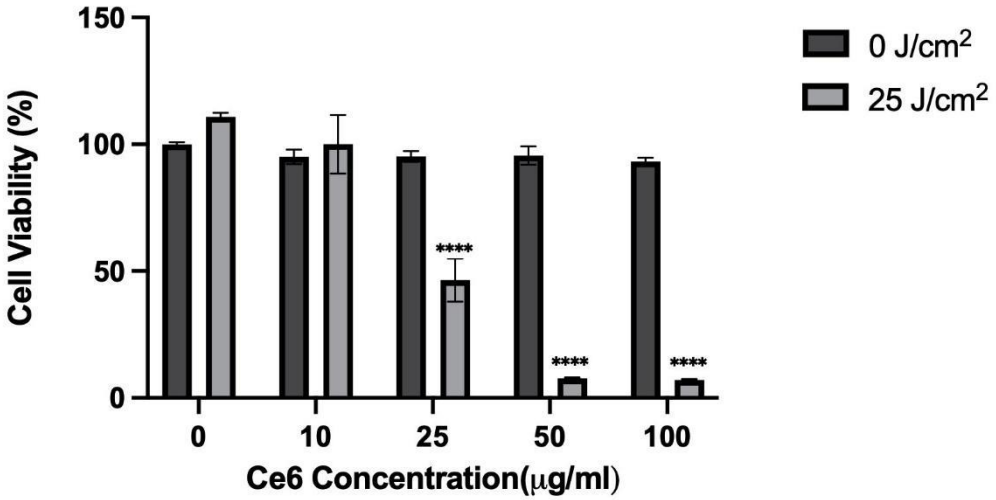

Figure 3.2: Cell viability analysis of 0, 10, 25, 50, and 100 μM of Ce6 concentrations after 1 incubation time. Each bar represented the average of the normalized with respect to the control group.

3.3 Intracellular Reactive Oxygen Species Production in Skov-3 Cells after PDT Applications

This study examined the generation of intracellular reactive oxygen species (ROS) in Skov-3 cells by using a DCFH-DA probe after undergoing Ce6-mediated PDT applications with a 655nm diode laser and the result is shown in Figure 3.3. The levels of reactive oxygen species (ROS) were measured in different conditions: absence of any treatment (0), exposure to laser light alone (0+L), and the combination of various concentrations of the photosensitizer Ce6 (10, 25, 50, and 100 μg/ml) with laser light exposure (25 J/cm²).

As depicted in (Figure 3.3), the initial amount of reactive oxygen species (ROS) in cells that were not treated was designated as the baseline value (1.0). Exposure to laser light alone (0+L) had a 4.9% ROS production and it did not have a significant impact on ROS levels compared to the untreated control. Similarly, the levels of reactive oxygen species (ROS) in cells treated with 10 and 25 μg/ml Ce6 and photodynamic

therapy (PDT) did not show a significant difference and it showed 4.97 and 5.47% compared to the untreated control. At concentrations of 50 μg/ml and 100 μg/ml Ce6, there was a significant and noticeable increase in the formation of reactive oxygen species (ROS), with the ROS levels increasing roughly to 28.3 and 42.2% when compared to the control level, respectively (**, $p < 0.0021$)(***, $p < 0.0002$)(****, $p < 0.0001$).

These findings were subsequently validated through statistical comparisons among different treatment groups. The study observed notable disparities in reactive oxygen species (ROS) levels when comparing lower and higher concentrations of Ce6. These findings were subsequently validated through statistical comparisons among different treatment groups. The study observed notable disparities in reactive oxygen species (ROS) levels when comparing lower and higher concentrations of Ce6. This emphasizes the impact of Ce6-mediated photodynamic therapy (PDT) on ROS generation in Skov-3 cells, which is dependent upon the dosage of Ce6.

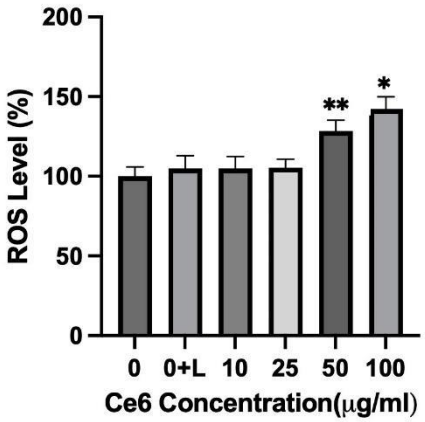

Figure 3.3: Reactive oxygen species formation after 655-nm 25J/cm2 energy densities density after 1h incubation. Photosensitizer concentrations: 10, 25, 50, and 100 μM of Ce6.

3.4 Reactive Oxygen Species Generation Capacity of Chlorin e6

1,3-Diphenylisobenzofuran (DPBF) is a chemical probe used to detect ROS, particularly singlet oxygen ($^1O2$). DPBF reacts with singlet oxygen to form an endoperoxide, which results in a decrease in its characteristic absorbance at around 410 nm. The goal of the experiment was to assess the ability of 100 μM Ce6 to generate reactive oxygen species (ROS) with different laser power levels (100, 200, 300, and 400 mW) on the production of reactive oxygen species (ROS) using a 655 nm laser for 30 seconds. The results, shown in Figure 3.4, reveal a clear power-dependent increase in ROS formation.

At 100 mW, the absorbance peak around 410 nm shows a minor decrease compared to the control, indicating 5.7% in ROS production. Increasing the power to 200 mW results in a more significant reduction in absorbance, indicating 60% in ROS production. At 300 mW and 400 mW, the absorbance decreases further, indicating higher ROS production, with 400 mW showing the most substantial ROS generation and it showed 123% ROS production compared to control.

The second experiment examined the ability of Ce6 to generate reactive oxygen species (ROS) at various concentrations (10, 25, 50, and 100 μM) using a 655 nm laser with an energy density of 25 J/cm² delivered for 3 minutes and 15 seconds. The absorbance spectra demonstrate a concentration-dependent rise in the production of reactive oxygen species (ROS). More precisely, the absorbance peak at approximately 410 nm (which is indicative of DPBF) diminishes as the concentration of Ce6 increases, implying a greater generation of reactive oxygen species (ROS) at higher Ce6 concentrations. At 10 μM Ce6, the absorbance shows a minor reduction compared to the control (DPBF only) and showed 67.76% ROS generation. As the concentration increases to 25 μM and 50 μM, a noticeable decrease in absorbance is observed, indicating moderate ROS production, and the ROS generation percentage reached 84 and 93 compared to the control group. At 100 μM Ce6, the absorbance is significantly reduced, indicating the highest ROS production among the tested concentrations and it gives us a great number of 106% in ROS generation. This trend validates the relationship between the generation of reactive oxygen species (ROS) by Ce6 and its

concentration, where larger concentrations result in a greater production of ROS when exposed to the specified laser irradiation circumstances. with the help of these findings, we can emphasize the fact that ROS production is highly dependent on Ce6 concentration along with the power of the laser irradiation, with higher laser power or Ce6 concentration resulting in greater ROS production.

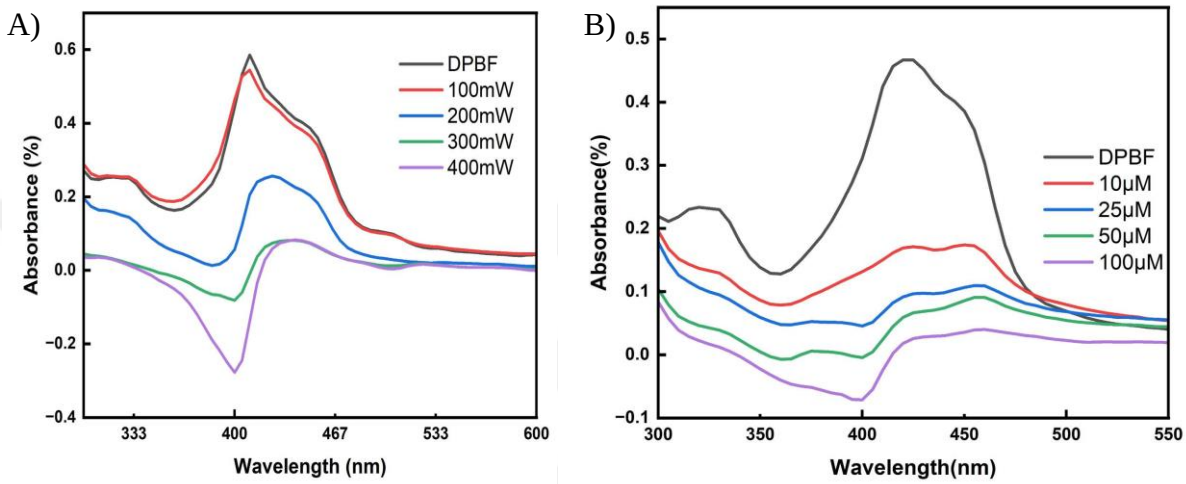

Figure 3.4: Absorbance spectrum of A)100 μM Ce6 with different laser power different laser power levels (100, 200, 300, and 400 mW) and B) different Ce6 concentrations (10, 25, 50, and 100 μM) using a 655 nm laser with an energy density of 25 J/cm²

3.5 Electrochemical Sensor Analysis to Determine the Reactive Oxygen Species Generation Capacity of Chlorin e6

Differential Pulse Voltammetry (DPV) is an electrochemical method employed for the examination of the redox characteristics of chemical compounds. DPV involves the addition of a sequence of potential pulses to a linear potential sweep, and the current is measured immediately before the application of each pulse. This method improves the sensitivity and accuracy of the test by minimizing the impact of the charging current, making it ideal for detecting small amounts of electroactive substances. we

can infer the efficiency of ROS production by Ce6 under laser illumination. The DPV technique enables the measurement of reactive oxygen species (ROS) production by Ce6 in the presence of laser light. As the production of ROS increases, the oxidation of HQ to BQ also increases, leading to a more pronounced DPV signal.

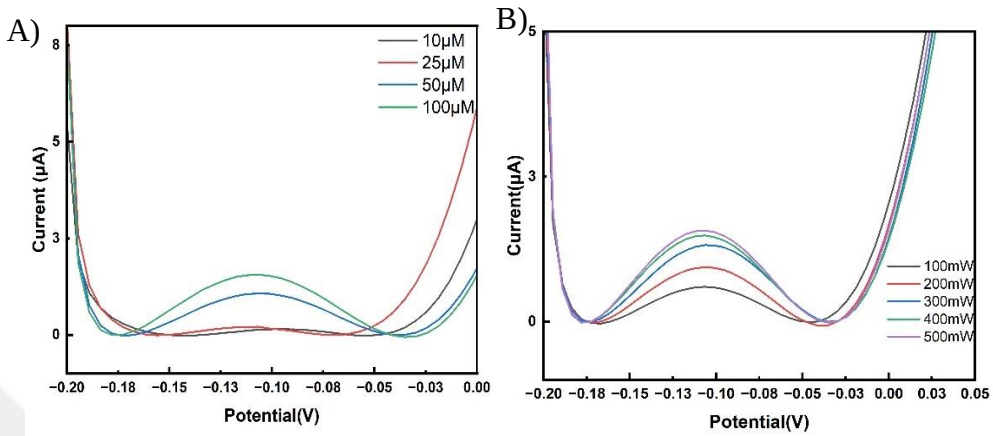

Figure 3.5: DPV curve obtained from A) different Ce6 concentrations B) different Laser power

Figure 3.5 shows the DPV signals from samples with different concentrations of Ce6 under a 655 nm laser. The signals show a baseline level of current, indicating minimal ROS production. The signal slightly increases with Ce6 concentration, indicating a small amount of ROS generation. A noticeable peak in the current indicates a moderate increase in ROS production. The highest current peak indicates substantial ROS generation. This indicates a concentration-dependent increase in ROS production, consistent with absorbance data. Similar to the concentration-dependent data, the increasing current peaks with higher laser power suggest a power-dependent increase in ROS generation. This result aligns with the absorbance data, confirming that higher laser power enhances ROS production by Ce6 under the specified conditions.

Chronoamperometry (CA) was used to analyze the generation of reactive oxygen species (ROS) in mixtures of 100μM Chlorin e6 (Ce6) and hydroquinone (HQ) under laser light. Figure 3.6 provided insights into the electrochemical behavior of the system and the efficiency of ROS production under different laser powers and varying Ce6 concentrations. The results showed a strong linear relationship between Ce6 concentration and different laser powers with ROS production, with a specific equation

indicating that as Ce6 concentration or laser power increases, the current (reflecting ROS production) decreases linearly. The fitting curve for the laser power-dependent linear relationship (R^2 = 0.932) and for concentration-dependent current response shows a strong linear relationship (R^2 = 0.942), suggesting a clear correlation between Ce6 concentration and different laser power with ROS production. The high fitting curve seen in the fitting curves provides strong evidence for the dependability of the results. This indicates that the current response, which reflects the formation of reactive oxygen species (ROS), can be accurately anticipated based on the concentration of Ce6 and laser powers.

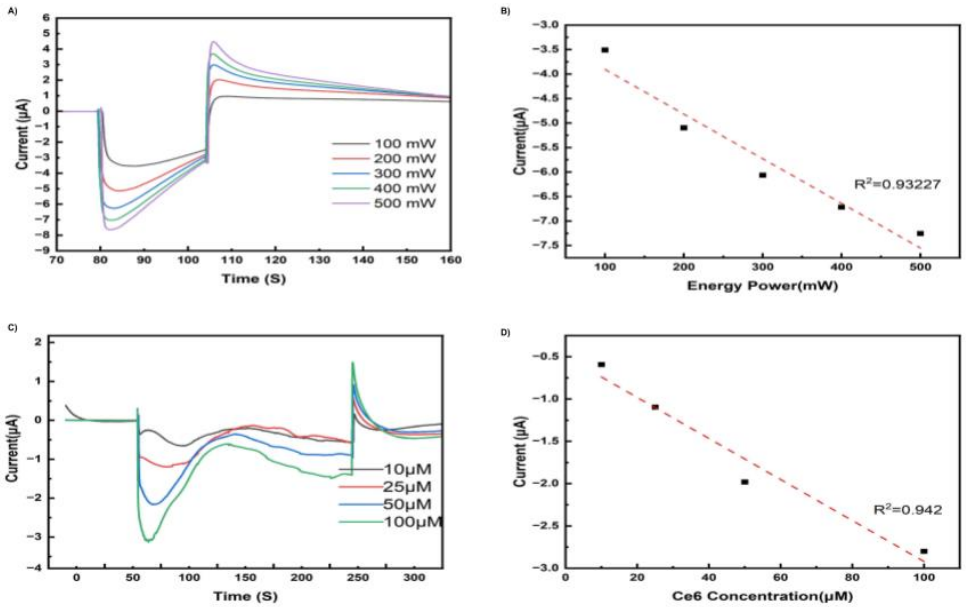

Figure 3.6: Chronoamperometry (CA) curve obtained from A)100 μM Ce6 mixed with HQ under different laser B) together with a calibration curve and Chronoamperometry (CA) curve obtained from C) different Ce6 concentration under 500 mW laser power with an energy density of 25 J/cm² D) together with a calibration curve

3.6 Electrochemical Sensor Analysis to Determine the Intracellular Reactive Oxygen Species Production

To effectively monitor the release of ROS from cancer cells, the sensor was designed to incorporate chronoamperometry, which enhances sensitivity and eliminates the

need for scanning high overpotentials. Figure 3.7A displays the cyclic voltammetry(CV) reactions of the SPE sensors under various applied potentials ranging from -0.4 to +0.4 V. In order to see the CV reaction and change under different conditions we get the result before applying the laser and during laser application with 500mW. To balance the need for a low overpotential and the desired signal, a potential of -0.05 V was selected for further investigations.

Chronoamperometry was carried out to obtain detailed information about the production of Reactive Oxygen Species (ROS) throughout time. Chronoamperometry is a technique used to quantify the current response over some time following a sudden shift in electrical potential. This method is particularly useful for monitoring dynamic processes, such as the formation of reactive oxygen species (ROS). The current-time curves exhibited obvious differences across the different Ce6 concentrations, with greater concentrations resulting in more pronounced decreases in current. The fitting curve demonstrates a good linear correlation (R^2 = 0.98698), indicating a direct association between Ce6 concentration and ROS generation.

At concentrations of 100 μM, there was a significant and noticeable increase in the formation of reactive oxygen species (ROS), with the ROS levels increasing roughly to 80% when compared to the 0μM Ce6 concentration, respectively. This number reaches 71 and 56% for 50 and 25 μM Ce6 concentration (Figure 3.7).

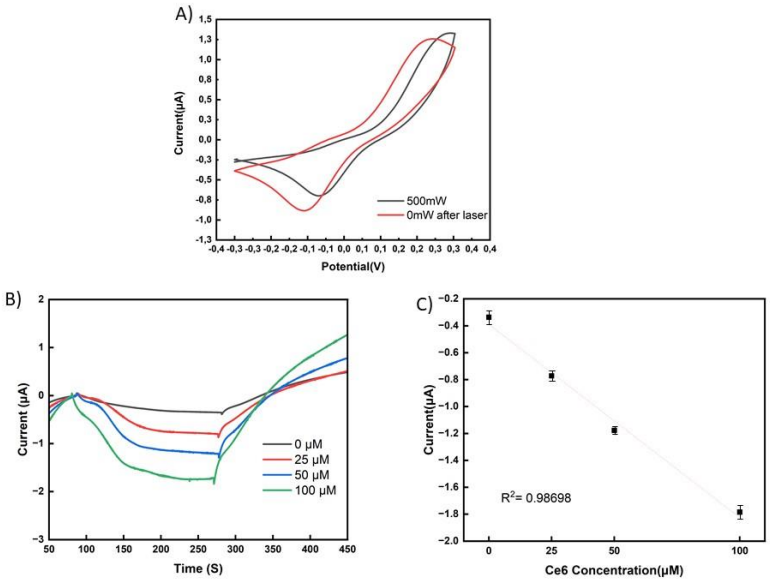

Figure 3.7: A) CV curve from Skov-3 cancer cells incubated with 100 μM Ce6 mixed with HQ before and after 500 mW laser B) CA curve obtained from Skov-3 cancer cells incubated with different Ce6 concentrations after 25 J/cm^2 laser C) together with it's calibration curve

Chapter 4

Discussion

The conventional approach for managing SKOV-3 ovarian cancer normally entails surgical removal of the tumor together with supplementary medicines aimed at destroying any remaining cancer cells.

Although chemotherapy and radiation are frequently employed, the reappearance of tumors continues to be a substantial obstacle, especially in advanced stages. Recurrence commonly arises from multiple factors, including the challenge of administering therapeutic doses without causing severe side effects, as well as the emergence of resistance in both cancer cells and cancer stem cells [22, 24]. Cancer remains a leading global health issue, responsible for millions of deaths annually. Traditional treatments like surgery, chemotherapy, and radiation therapy often come with severe side effects and limitations on patients' quality of life. Photodynamic Therapy (PDT) has emerged as a promising alternative, using photosensitizers as a light-sensitive drug to generate reactive oxygen species (ROS) that induce apoptosis in cancer cells upon light activation [37]. Effective PDT relies on the accurate detection of ROS to ensure sufficient production for tumor destruction without harming surrounding healthy tissues [40]. While conventional ROS detection kits can be inaccurate due to biological interference, electrochemical sensors, particularly screen-printed electrodes (SPEs), offer a cost-effective, portable, and sensitive method for real-time ROS monitoring. This advancement could significantly enhance PDT efficacy and cancer treatment outcomes by allowing precise optimization of therapy protocols [68].

The study's findings illustrate the possibility of PDT as a feasible substitute for traditional cancer therapies. Through the utilization of Ce6 as a photosensitizer and the application of laser irradiation, major quantities of reactive oxygen species (ROS) were produced, playing a crucial role in triggering apoptosis in cancer cells. The results revealed a distinct link between the level of Ce6 concentration and the quantity of ROS generated, with greater concentrations resulting in a more significant production of ROS [66]. This was evidenced by both the increased fluorescence intensity of the

DCFH-DA probe and the reduction in DPBF absorbance post-irradiation. ROS plays a pivotal role in the mechanism of PDT. Upon activation by laser light, Ce6 generates ROS, including singlet oxygen, superoxide radicals, and hydroxyl radicals. These reactive species cause oxidative damage to cellular macromolecules such as lipids, proteins, and DNA, leading to apoptosis or necrosis of cancer cells. The study confirmed that higher ROS levels correspond to increased cytotoxic effects on SKOV-3 cells, especially at higher concentrations of Ce6 [39]. The main aim of this work was to assess the generation of reactive oxygen species (ROS) within SKOV-3 ovarian cancer cells when treated with different concentrations of Chlorin e6 (Ce6) and exposed to laser light. The electrochemical changes related to the formation of reactive oxygen species (ROS) were monitored using electrochemical sensors, namely Differential Pulse Voltammetry (DPV) and Chronoamperometry (CA). The research on the impact of laser irradiation on SKOV-3 cells offers significant knowledge regarding the survival of these cells under photodynamic therapy (PDT) conditions with an energy density of 25 J/cm². The study showed that exposure to this energy density did not have a significant effect on the survival of cells, hence emphasizing key components of photodynamic therapy (PDT) and its interaction with cancer cells. Photodynamic therapy utilizes the combined effects of a photosensitizing drug, light, and molecular oxygen to generate cytotoxic reactive oxygen species (ROS) that can cause cell death. The procedure generally entails the application of a photosensitizer, exposure to a certain light wavelength, and the production of reactive oxygen species (ROS).

In this work, SKOV-3 cells were subjected to laser light with an energy density of 25 J/cm², without the use of a photosensitizer. This led to a small rise in cell viability (10.85%) compared to the control group. This indicates that laser light alone, at this level of energy density, does not cause substantial cytotoxic effects. The results emphasize the significance of the photosensitizer in photodynamic therapy (PDT), as the interaction between the photosensitizer and light is essential for the formation of reactive oxygen species (ROS). Hence, it is crucial to optimize the concentration of photosensitizer, the dosage of light, and the duration of exposure to maximize therapeutic results while minimizing any negative consequences.

By investigating the cytotoxic effects of Ce6 on SKOV-3 human ovarian cancer cells

during photodynamic treatment (PDT) with an energy density of 25 J/cm², we indicated that Ce6 alone did not demonstrate substantial cytotoxicity, suggesting that its cytotoxic effects are specifically triggered by exposure to light during PDT. Nevertheless, when subjected to PDT at an intensity of 25 J/cm², there was a significant decrease in the survival rate of cells, which was directly linked to the amount of Ce6 present. The data exhibited a visible reduction in cell viability as the concentrations of Ce6 increased during PDT, suggesting a cytotoxic impact that is dependent on the dosage. The harmful effects of Ce6-mediated photodynamic therapy (PDT) can be ascribed to the production of reactive oxygen species (ROS) when light is activated [69]. The primary processes and mechanisms of action include the activation of photosensitizers, intersystem crossover, the production of reactive oxygen species (ROS), and subsequent cellular damage.

$$\text{Ce6 (Triplet State)} + O2 \rightarrow \text{Ce6} + {}^1O2$$

$$^1O2 + H2O \rightarrow 2\ \bullet OH + 2\ H^+$$

The generated ROS causes oxidative damage to cellular components, including lipids, proteins, and nucleic acids. This oxidative stress leads to apoptosis or necrosis of the cancer cells. The decrease in cell viability, which is dependent on the concentration, indicates that it is essential to optimize the concentration of Ce6 to maximize the therapeutic effectiveness of PDT. Increased concentrations of Ce6 result in higher levels of reactive oxygen species (ROS) production, which in turn leads to more pronounced cytotoxic effects. Nevertheless, it is crucial to maintain a proper equilibrium in the concentration of photosensitizer to prevent any potential harm to adjacent healthy tissues [70]. For examining the production of intracellular reactive oxygen species (ROS) in SKOV-3 cells after Ce6-mediated photodynamic therapy (PDT), we used the ROS-sensitive probe 2′,7′-Dichlorofluorescein diacetate (DCFH-DA) which facilitated proper estimates of ROS levels, uncovering important discoveries regarding the cellular reactions to PDT. DCFH-DA is a lipophilic chemical that can readily pass through cell membranes and it is non-fluorescence. Upon entering the cells, it is subjected to deacetylation by cellular esterases, resulting in the formation of 2′,7′-Dichlorofluorescein (DCFH), which remains non-fluorescent. When reactive oxygen species (ROS) are present, the molecule DCFH undergoes oxidation and transforms into the highly fluorescent chemical 2′,7′-Dichlorofluorescein (DCF). The

fluorescence intensity of DCF is directly proportional to the quantities of reactive oxygen species (ROS) present in the cells, enabling precise evaluation of intracellular ROS generation [72]. The initial amount of reactive oxygen species (ROS) in cells that were not treated with any drugs was established as 1.0. Exposure to laser light alone (0+L) led to a slight rise (4.9%) in reactive oxygen species (ROS), suggesting that laser light at 25 J/cm² did not considerably stimulate ROS production in the absence of a photosensitizer. The ROS levels following PDT for 10 and 25 μg/ml concentrations were 4.97% and 5.47%, respectively. These values were not substantially different from the control, indicating that there was limited production of ROS at these lower concentrations. An obvious increase in reactive oxygen species (ROS) generation was noted, with ROS levels escalating to around 28.3% and 42.2% respectively, in comparison to the control in 50 and 100μg/ml. The increase in reactive oxygen species (ROS) levels at elevated Ce6 concentrations can be attributed to various processes occurring both intracellularly and extracellularly.

The study reveals that the fluorescence intensity of Ce6 significantly increases, indicating that the increased oxygen can be converted into ROS under 655 nm laser irradiation can generate 1O2, resulting in the production of singlet oxygen, which can trigger lipid peroxidation, protein oxidation, and DNA damage [71]. Superoxide anions and hydroxyl radicals are additional reactive oxygen species (ROS) produced by subsequent reactions involving singlet oxygen and biological components, leading to oxidative stress and cellular damage. This damage disrupts the balance inside cells, causing cell death by apoptosis or necrosis, resulting in decreased cell viability [73]. Ce6-PDT induces both autophagy and apoptosis Skov-3 cancer cells. The study found that Ce6-PDT leads to a dose-dependent decrease in cell viability and induces apoptosis via the mitochondrial pathway [74].

Investigating the production of reactive oxygen species (ROS) by chlorine e6 (Ce6) using 1,3-diphenylisobenzofuran (DPBF) as a chemical probe gives us the following results. DPBF reacts with singlet oxygen to form an endoperoxide, which reduces its absorbance at 410 nm, serving as a reliable indicator of singlet oxygen generation. When DPBF encounters singlet oxygen, it undergoes a chemical reaction to form 1,2-dibenzoylbenzene, causing a decrease in its characteristic absorbance at 410 nm. Ce6 samples (10, 25, 50, and 100 μM) were irradiated with a 655 nm diode laser, and the

absorbance at 410 nm was measured before and after irradiation to quantify singlet oxygen production. in 10 μM Ce6 a minor reduction in absorbance, corresponding to 67.76% ROS generation compared to the control was obtained. for 25 μM and 50 μM Ce6 we Demonstrated moderate reductions in absorbance, indicating increased ROS production, with ROS generation percentages of 84 and 93, respectively. 100 μM Ce6 Showed the most significant reduction in absorbance, indicating the highest ROS production at 106% compared to the control.

These results illustrate a clear concentration-dependent increase in ROS production, validating that higher concentrations of Ce6 result in greater singlet oxygen generation when exposed to laser irradiation. for 100mw Power application Minor decrease in absorbance, indicating 5.7% ROS production. for 200 mW More significant absorbance reduction, indicating 60% ROS production. when it reached 300 mW and 400 mW Further decreases in absorbance, with 400 mW showing the most substantial ROS generation at 123% compared to the control.

These results indicate 1O2 production of PDT in a power and dose-dependent manner. , it is believed that further increasing the amount of Ce6 would induce more 1O2 generation [75] Mitochondria and low levels of reactive oxygen species (ROS) can have a crucial impact on maintaining cellular balance by influencing cellular signaling pathways. On the other hand, when there are high levels of reactive oxygen species (ROS) and the equilibrium between production and scavenging is disrupted, oxidative stress arises. This results in non-selective harm to biological molecules, as well as a breakdown of cellular processes, and ultimately leads to cell death. Our research indicated that radiation exposure can cause an increase in the formation of reactive oxygen species (ROS). Specifically, there was an increase in the generation of reactive oxygen species (ROS) following exposure to 400 mW of radiation [76]. Continuing our ROS detection experiment, we examine the efficiency of reactive oxygen species (ROS) production by Chlorin e6 (Ce6) under laser illumination using Differential Pulse Voltammetry (DPV) and Chronoamperometry (CA). The results show a clear correlation between Ce6 concentration, laser power, and ROS production.

DPV is an electrochemical technique that enhances sensitivity and accuracy by reducing the influence of the charging current. This makes it particularly useful for detecting small quantities of electroactive substances, such as ROS. In this study, DPV

was employed to measure ROS production by Ce6 under laser illumination. Samples with different concentrations of Ce6 under a 655 nm laser showed minimal ROS production without significant laser power or Ce6 concentration. An increase in Ce6 concentration led to a corresponding increase in ROS generation, indicating that higher concentrations of Ce6 enhance ROS generation.

The DPV signals also demonstrated a power-dependent increase in ROS production. Higher laser power resulted in more substantial ROS generation, consistent with the absorbance data. This suggests that laser power is a critical factor in optimizing ROS production by Ce6. It is thus evident from the graph that the amperometric response towards the Production of ROS is linear ($R^2 = 0.942$) between Ce6 concentration and ROS and ($R^2 = 0.932$) was observed between laser power and ROS production. Moreover, higher laser power resulted in more substantial ROS generation, suggesting that laser power is a critical factor in optimizing ROS production by Ce6. The study also found a strong linear relationship between Ce6 concentration and ROS production, indicating the importance of using Ce6 concentration as a predictor of ROS generation. the response of the sensor to varying Dose and Power parameters is confirmed by the suppression of the signal which detects the amount of ROS production. Hydroquinone (HQ) and similar phenols exhibit reversible electrochemistry, which involves the transfer of two electrons and two protons. Hydroquinone (HQ) can undergo oxidation to form benzoquinone (BQ) in the presence of photogenerated singlet oxygen (1O2). Applying a suitable negative voltage at the electrode surface allows for the reduction of BQ back to HQ. A redox cycle activated by light generated a photocurrent that varied according to the concentration of the phenol in the solution [64]. Evidence is accumulating that the generation of reactive oxygen species (ROS) is intimately associated with the photodynamic effect of many sensitizers involved in cancer therapy. While 1O2 is believed to be the major mediator of photochemical cell damage for many types of photosensitizers, oxygen species like the superoxide anion and the hydroxyl radical (•OH) can also induce deleterious effects including lipid peroxidation and membrane damage [65].

with the help of the provided data, we succeeded in the aftermath of the Production of ROS, and by utilizing an electrochemical sensor designed with chronoamperometry

we monitored the release of Reactive Oxygen Species (ROS) from cancer cells. The selection of this method was based on its ability to increase sensitivity and avoid the requirement for significant overpotentials, which can introduce complexity to measurements and impact the precision of outcomes. By varying the potential within the range of -0.4 to +0.4 V, it was found that a potential of -0.05 V achieved the best compromise between minimizing overpotential and obtaining the desired signal. This potential value established a stable baseline for subsequent experiments. Chronoamperometry was used after Differential Pulse Voltammetry (DPV) to conduct a thorough examination of the generation of Reactive Oxygen Species (ROS) throughout time. Understanding the dynamics of ROS formation over time is essential for studying the metabolic activities and oxidative stress responses in cancer cells. The chronoamperometric current-time curves showed important variations at different Ce6 concentrations, with greater concentrations leading to more pronounced declines in current.

The study revealed a strong linear correlation (R^2 = 0.98698) between Ce6 concentration and ROS production, indicating that the electrochemical sensor effectively quantifies ROS levels. At a concentration of 100 µM Ce6, ROS levels increased by approximately 80% compared to the 0 µM control. This significant rise in ROS production underscores the sensitivity of the sensor and its capability to detect even subtle changes in ROS levels.

The regulation of cellular redox homeostasis involves maintaining a balance between the production of reactive oxygen species (ROS) and their removal through the ROS scavenging system. Therefore, it is beneficial to measure both the formation of reactive oxygen species (ROS) and the level of antioxidants in a single living cell at the same time. This allows for the correlation of their changes and the assessment of the cell's oxidative status during oxidative stress [77].

This study compares the effectiveness of Photodynamic Therapy (PDT) with ROS detection probes and an electrochemical sensor based on Screen-Printed Electrodes (SPE) in SKOV-3 cells. The SPE-based electrochemical sensor demonstrated superior ROS detection and higher ROS production signals. The PDT method uses a photosensitizer (Ce6) activated by laser light, leading to ROS production. ROS levels are detected using fluorescent probes like DCFH-DA, which emit fluorescence upon

reacting with ROS. However, this method offers only discrete snapshots of ROS levels rather than continuous monitoring.

The SPE-based electrochemical sensor demonstrated a clear and significant increase in current at -0.05V upon laser irradiation, indicating enhanced ROS production. Current-time curves exhibited a strong linear correlation between Ce6 concentration and ROS generation, demonstrating the sensor's sensitivity and accuracy. Higher ROS signals were observed in the sensor experiment, with ROS levels increasing by approximately 80% at 100 μM Ce6 compared to the control, and significant increases at 50 μM and 25 μM Ce6 concentrations.

The advantages of SPE-based electrochemical sensors for ROS detection include continuous monitoring, high sensitivity and specificity, quantitative accuracy, enhanced signal detection, reduced interference and noise, cost-effectiveness, versatility, and portability. These advantages make SPE-based sensors suitable for widespread use, disposable applications, and on-site and real-time analysis without the need for sophisticated laboratory equipment.

Chapter 5

Conclusion

This study explores the effectiveness of reactive oxygen species (ROS) detection in cancer research and therapy. The researchers used two primary methods: Photodynamic Therapy (PDT) with ROS detection probes and an electrochemical sensor based on Screen-Printed Electrodes (SPE). The SPE-based electrochemical sensor demonstrated superiority in terms of sensitivity, specificity, and real-time monitoring capabilities.

PDT involves activating a photosensitizer by light in the presence of oxygen, leading to ROS production. This method utilizes fluorescent probes, such as DCFH-DA, which emit fluorescence upon reacting with ROS. The intensity of fluorescence directly correlates with the amount of ROS generated, providing a quantifiable measure of ROS levels. However, PDT primarily offered discrete time-point measurements, restricting the ability to monitor dynamic changes in ROS levels continuously.

The electrochemical sensor incorporating SPE was designed to provide continuous monitoring of ROS production using chronoamperometry. A potential of -0.05V was selected based on cyclic voltammetry (CV) signal analysis to optimize sensitivity and minimize noise. The sensor utilized Ce6 as a photosensitizer and hydroquinone (HQ) as a ROS scavenger to ensure the specificity of the electrochemical signals to ROS activity.

The SPE-based electrochemical sensor offers several advantages over traditional PDT with ROS detection probes. It offers continuous monitoring, high sensitivity and specificity, quantitative accuracy, enhanced signal detection, reduced interference and noise, and cost-effectiveness. The sensor's ability to capture subtle changes in ROS levels continuously provides a more detailed and accurate picture of ROS activity.

SPE-based sensors are also cost-effective, versatile, and portable, enabling on-site and real-time analysis without the need for sophisticated laboratory equipment. This portability is particularly advantageous for field studies and point-of-care diagnostics.

In conclusion, the SPE-based electrochemical sensor approach for ROS detection in SKOV-3 cells offers significant advantages over traditional PDT with ROS detection probes. The ability to continuously monitor ROS production, combined with higher sensitivity, specificity, and quantitative accuracy, makes SPE-based electrochemical sensors a superior choice for ROS detection. The enhanced ROS signals observed in the sensor experiment underscore its effectiveness in capturing dynamic changes in ROS levels, providing valuable insights for cancer research and therapy optimization.

Accurate and reliable ROS detection is critical for understanding the role of ROS in cancer and other diseases. Advancements in electrochemical sensor technology, particularly the use of SPE, represent a significant step forward in ROS research. By minimizing errors and providing higher sensitivity, SPE-based sensors ensure more precise and actionable data, ultimately contributing to better outcomes in biomedical research and clinical practice.

References

[1] Tarin, D. (2023). Understanding cancer: The molecular mechanisms, biology, pathology and clinical implications of malignant neoplasia. Springer.

[2] Macdonald, F., Ford, C., & Casson, A. (2004). Molecular biology of cancer. Garland Science.

[3] Tan, W., & Hanin, L. (2008). Handbook of cancer models with applications. CRC Press.

[4] Williams, G. H., & Stoeber, K. (2011). The cell cycle and cancer. Nature Reviews Cancer, 11(4), 231-241. https://doi.org/10.1002/path.3022

[5] Fior, R., & Zilhão, R. (2019). Molecular and cell biology of cancer: When cells break the rules and hijack their planet. Springer International Publishing.

[6] Kamata, H., Honda, S., Maeda, S., Chang, L., Hirata, H., & Karin, M. (2005). Reactive oxygen species promote TNFα-induced death and sustained JNK activation by inhibiting MAP kinase phosphatases. Cell, 120(5), 649–661. https://doi.org/10.1016/j.cell.2004.12.041

[7] Thompson, C. B. (2011). Rethinking the regulation of cellular metabolism. Cold Spring Harbor Symposia on Quantitative Biology, 76, 23-29. https://doi.org 10.1101/sqb.2012.76.010496

[8] Zhang, J., Wang, X., Vikash, V., Ye, Q., Wu, D., Liu, Y., & Dong, W. (2016). ROS and ROS-mediated cellular signaling. Oxidative Medicine and Cellular Longevity, 2016, 1-18. https://doi.org/10.1155/2016/4350965

[9] Yang, Y., Karakhanova, S., Werner, J., & Bazhin, A. V. (2013). Reactive oxygen species in cancer biology and anticancer therapy. Current Medicinal Chemistry, 20(30), 3677-3692. https://doi.org/10.2174/09298673113209990302

[10] Chasara, R. S., & Ajayi, T. O. (2023). Exploring novel strategies to improve anti-tumor efficiency: The potential for targeting reactive oxygen species. International Journal of Molecular Sciences. Advance online publication. https://doi.org/10.1016/j.heliyon.2023.e19896

[11] Perillo, B., Di Donato, M., Pezone, A., Di Zazzo, E., Giovannelli, P., Galasso, G., Castoria, G., & Migliaccio, A. (2020). ROS in cancer therapy: The bright side of the moon. Experimental & Molecular Medicine, 52(2), 192–203. https://doi.org/10.1038/s12276-020-0384-2

[12] Farghaly, S. A. (2022). Advances in diagnosis and management of ovarian cancer. Springer. https://doi.org/10.1007/978-3-030-98165-9

[13] Banks, E., Beral, V., & Reeves, G. (1997). The epidemiology of epithelial ovarian cancer: A review. International Journal of Gynecological Cancer, 7(5), 425–438. https://doi.org/10.1046/j.1525-1438.1997.07567.x

[14] Bartlett, J. M. S. (2000). Ovarian cancer: Methods and protocols. Humana Press. https://doi.org/10.1385/1592591238

[15] Chi, D. S., Berchuck, A., Dizon, D. S., & Yashar, C. M. (Eds.). (2017). Principles and practice of gynecologic oncology (7th ed.). Wolters Kluwer Health.

[16] Gibson, E., & Mahdy, H. (2023). Anatomy, abdomen and pelvis, ovary. In StatPearls. StatPearls Publishing. https://www.ncbi.nlm.nih.gov/books/NBK482509/

[17] Seneda, M., Bergamo, L. Z., Miguez-Gonzalez, S., & Zangirolamo, A. F. (2022). Folliculogenesis in cattle. Animal Reproduction, 19(2), e20220028. https://doi.org/10.1590/1984-3143-AR2022-0028

[18] Wang, J. J., Lei, K. F., & Han, F. (2018). Tumor microenvironment: Recent advances in various cancer treatments. European Review for Medical and Pharmacological Sciences, 22(12), 3855–3864. https://doi.org/10.26355/eurrev_201806_15270

[19] Yun, J., Mullarky, E., Lu, C., et al. (2015). Vitamin C selectively kills KRAS and BRAF mutant colorectal cancer cells by targeting GAPDH. Science, 350(6266), 1391-1396. https://doi.org/10.1126/science.aaa5004

[20] Colombo, N., & Pecorelli, S. (2003). What have we learned from ICON1 and ACTION? International Journal of Gynecological Cancer, 13(Suppl 2), 140–143. https://doi.org/10.1046/j.1525-1438.2003.13352.x

[21] Chan, J. K., Tian, C., Teoh, D., Monk, B. J., Herzog, T., Kapp, D. S., & Bell, J. (2010). Survival after recurrence in early-stage high-risk epithelial ovarian cancer: A Gynecologic Oncology Group study. Gynecologic Oncology, 116(3), 307–311. https://doi.org/10.1016/j.ygyno.2009.10.073

[22] Mirza, M. R., et al. (2020). The forefront of ovarian cancer therapy: Update on PARP inhibitors. Annals of Oncology, 31(9), 1148–1159. https://doi.org/10.1016/j.annonc.2020.05.011

[23] Chi, D. S., Berchuck, A., Dizon, D. S., & Yashar, C. M. (Eds.). (2017). Principles and practice of gynecologic oncology (7th ed.). Wolters Kluwer Health.

[24] Lengyel, E. (2010). Ovarian cancer development and metastasis. American Journal of Pathology, 177(3), 1053–1064. https://doi.org/10.2353/ajpath.2010.100105

[25] Vergote, I., Tropé, C. G., Amant, F., et al. (2010). Neoadjuvant chemotherapy or primary surgery in advanced ovarian cancer. New England Journal of Medicine, 363(10), 943–953. https://doi.org/10.1056/NEJMoa0908806

[26] Henretta, M. S., Anderson, C. L., Angle, J. F., & Duska, L. R. (2011). It's not just for laparoscopy anymore: Use of insufflation under ultrasound and fluoroscopic guidance by interventional radiologists for percutaneous placement of intraperitoneal chemotherapy catheters. Gynecologic Oncology, 123(2), 342–345. https://doi.org/10.1016/j.ygyno.2011.07.033

[27] Thirumaran, R., Prendergast, G. C., & Gilman, P. B. (2007). Cytotoxic chemotherapy in clinical treatment of cancer. In Cancer immunotherapy (pp. 101–116). Elsevier BV. https://doi.org/10.1016/B978-0-444-52249-7.00006-5

[28] Peng, Q., Juzeniene, A., Chen, J.-Y., Svaasand, L. O., Warloe, T., Giercksky, K. E., & Moan, J. (2008). Lasers in medicine. Reports on Progress in Physics, 71(5), 056701. https://doi.org/10.1088/0034-4885/71/5/056701

[29] Ortega-Martínez, R., Román-Moreno, C. J., & Rodríguez-Rosales, A. (2001). Review of applications of medical lasers. Journal of Photochemistry and Photobiology B: Biology, 61(1-2), 75-85. https://doi.org/10.1016/S1011-1344(01)00185-2

[30] Waidelich, R., & Waidelich, W. (2001). 40 years: Laser--a new light for medicine. Laser Florence: A Window on the Laser Medicine World, 4903, 40-46. https://doi.org/10.1117/12.472755

[31] Moan, J., & Peng, Q. (2003). European Society Photobiology. Photodynamic therapy (comprehensive series in photochemical and photobiological sciences). In Photodynamic therapy: An outline of the history of PDT (pp. 1–9). The Royal Society of Chemistry. https://doi.org/10.1039/9781847551628

[32] McDonagh, A. F. (2001). Phototherapy: From ancient Egypt to the new millennium. Journal of Perinatology, 21(1), 7–12. https://doi.org/10.1038/sj.jp.7200443

[33] Abdel-Kader, M. H. (2014). Photodynamic therapy: From theory to application. Springer-Verlag Berlin Heidelberg. https://doi.org/10.1007/978-3-642-39768-7

[34] Yoon, I., Li, J., & Shim, Y. K. (2013). Advance in photosensitizers and light delivery for photodynamic therapy. Clinical Endoscopy, 46(1), 7-23. https://doi.org/10.5946/ce.2013.46.1.7

[35] Dolmans, D. E., Fukumura, D., & Jain, R. K. (2003). Photodynamic therapy for cancer. Nature Reviews Cancer, 3(5), 380–387. https://doi.org/10.1038/nrc1071

[36] Jori, G. (1996). Tumor photosensitizers: Approaches to enhance the selectivity and efficiency of photodynamic therapy. Journal of Photochemistry and Photobiology B: Biology, 36(2), 87–93. https://doi.org/10.1016/1011-1344(96)07307-4

[37] Ochsner, M. (1997). Photophysical and photobiological processes in the photodynamic therapy of tumors. Journal of Photochemistry and Photobiology B: Biology, 39(1), 1–8. https://doi.org/10.1016/S1011-1344(96)07307-4

[38] Niculescu, A.-G., & Grumezescu, A. M. (2021). Photodynamic therapy—An up-to-date review. Applied Sciences, 11(8), 3626. https://doi.org/10.3390/app11083626

[39] Dąbrowski, J. M. (2016). Reactive oxygen species in photodynamic therapy. Journal of Photochemistry and Photobiology B: Biology, 164, 251-266. https://doi.org/10.1016/j.jphotobiol.2016.08.012

[40] Zhou, Z., Song, J., Nie, L., & Chen, X. (2016). Reactive oxygen species generating systems meeting challenges of photodynamic cancer therapy. Chemical Society Reviews, 45(23), 6597–6626. https://doi.org/10.1039/c6cs00271d

[41] Fitzgerald, F. (2017). Photodynamic therapy (PDT). Nova Science Publishers, Inc.

[42] Castano, A. P., Demidova, T. N., & Hamblin, M. R. (2004). Mechanisms in photodynamic therapy: Part one—Photosensitizers, photochemistry and cellular localization. Photodiagnosis and Photodynamic Therapy, 1(4), 279-293. https://doi.org/10.1016/S1572-1000(05)00007-4

[43] Hak, A., Ali, M. S., Sankaranarayanan, S. A., Shinde, V. R., & Rengan, A. K. (2023). Chlorin e6: A promising photosensitizer in photo-based cancer nanomedicine. ACS Applied Bio Materials. https://doi.org/10.1021/acsabm.3c00407

[44] Yoon, I., Zhu, J. L., & Shim, Y. K. (2013). Advance in photosensitizers and light delivery for photodynamic therapy. Clinical Endoscopy, 46(1), 7-23. https://doi.org/10.5946/ce.2013.46.1.7

[45] Castano, A. P., Demidova, T. N., & Hamblin, M. R. (2004). Mechanisms in photodynamic therapy: Part one—Photosensitizers, photochemistry and cellular localization. Photodiagnosis and Photodynamic Therapy, 1(4), 279-293. https://doi.org/10.1016/S1572-1000(05)00007-4

[46] O'Connor, A. E., Gallagher, W. M., & Byrne, A. T. (2009). Porphyrin and nonporphyrin photosensitizers in oncology: Preclinical and clinical advances in photodynamic therapy. Photochemistry and Photobiology, 85(5), 1053-1074. https://doi.org/10.1111/j.1751-1097.2009.00585.x

[47] Fracchiolla, N., Artuso, S., & Cortelezzi, A. (2013). Biosensors in clinical practice: Focus on oncohematology. Journal of Sensors, 2013, 1–10. https://doi.org/10.1155/2013/149832

[48] Li, M., Li, R., Li, C. M., & Wu, N. (2011). Electrochemical and optical biosensors based on nanomaterials and nanostructures: A review. Frontiers in Bioscience (Scholar Edition), 3(2), 1308–1331. https://doi.org/10.2741/240

[49] Maruccio, G., & Narang, J. (2022). Electrochemical sensors: From working electrodes to functionalization and miniaturized devices. Elsevier. https://doi.org/10.1016/B978-0-12-821122-9.00001-1

[50] Lima, E., & Reis, L. V. (2023). Photodynamic therapy: From the basics to the current progress of N-heterocyclic-bearing dyes as effective photosensitizers. Molecules, 28(13), 5092. https://doi.org/10.3390/molecules28135092

[51] Allison, R. R. (2014). Photodynamic therapy: Oncologic horizons. Future Oncology, 10(1), 123–142. https://doi.org/10.2217/fon.13.213

[52] O'Connor, A., Gallagher, W., & Byrne, A. (2009). Porphyrin and nonporphyrin photosensitizers in oncology: Preclinical and clinical advances in photodynamic therapy. Photochemistry and Photobiology, 85(5), 1053-1074. https://doi.org/10.1111/j.1751-1097.2009.00585.x

[53] Zhu, C., Yang, G., Li, H., Du, D., & Lin, Y. (2014). Electrochemical sensors and biosensors based on nanomaterials and nanostructures. Analytical Chemistry, 86(1), 229-241. https://doi.org/10.1021/ac402871y

[54] Ghorbani-Bidkorbeh, F. (2015). Electrochemical sensors and biosensors represent very promising tools in pharmaceutical sciences. Iranian Journal of Pharmaceutical Research, 14(3), 615–617. https://doi.org/10.22037/ijpr.2015.1700

[55] Hulanicki, A., Glab, S., & Ingman, F. (1991). Chemical sensors: Definitions and classification. Pure and Applied Chemistry, 63(9), 1247–1250. https://doi.org/10.1351/pac199163091247

[56] Chaubey, A., & Malhotra, B. D. (2002). Mediated biosensors. Biosensors and Bioelectronics, 17(6-7), 441–456. https://doi.org/10.1016/S0956-5663(01)00310-0

[57] Bard, A. J., Faulkner, L. R., & White, H. S. (2022). Electrochemical methods: Fundamentals and applications (3rd ed.). Wiley.

[58] Saputra, H. A. (2023). Electrochemical sensors: Basic principles, engineering, and state of the art. Monatshefte für Chemie - Chemical Monthly, 154(10), 1083–1100. https://doi.org/10.1007/s00706-023-03113-z

[59] García-Miranda Ferrari, A., Carrington, P., Rowley-Neale, S. J., & Banks, C. E. (2020). Electroanalytical overview: Screen-printed electrochemical sensing platforms for the detection of vital cardiac, cancer, and inflammatory biomarkers. Environmental Science: Water Research & Technology, 6(10), 2676–2690. https://doi.org/10.1039/D0EW00637G

[60] Costa-Rama, E., & Fernández-Abedul, M. (2021). Paper-based screen-printed electrodes: A new generation of low-cost electroanalytical platforms. Biosensors, 11(11), 413. https://doi.org/10.3390/bios11110413

[61] Crapnell, R. D., García-Miranda Ferrari, A., Dempsey, N. C., & Banks, C. E. (2020). Electroanalytical overview: Screen-printed electrochemical sensing platforms for the detection of vital cardiac, cancer and inflammatory biomarkers. Environmental Science: Water Research & Technology, 6(10), 2676–2690. https://doi.org/10.1039/D0EW00637G

[62] Niu, P., Li, F., & Liang, X., et al. (2018). A porous polyaniline nanotube sorbent for solid-phase extraction of the fluorescent reaction product of reactive oxygen species in cells, and its determination by HPLC. Microchimica Acta, 185(10), 468. https://doi.org/10.1007/s00604-018-2954-0

[63] Kour, R., Arya, S., Young, S., Gupta, V., Bandhoria, P., & Khosla, A. (2020). Review—Recent advances in carbon nanomaterials as electrochemical biosensors. Journal of the Electrochemical Society, 167(3), 037555. https://doi.org/10.1149/1945-7111/ab7f0e

[64] Verrucchi, M., Giacomazzo, G., Sfragano, P. S., Laschi, S., Conti, L., Pagliai, M., Gellini, C., Ricci, M., Ravera, E., Valtancoli, B., Giorgi, C., & Palchetti, I. (2022). Characterization of a ruthenium(II) complex in singlet oxygen-mediated photoelectrochemical sensing. Langmuir, 38(29), 8881–8891. https://doi.org/10.1021/acs.langmuir.2c00875

[65] Rajendran, M. (2016). Quinones as photosensitizer for photodynamic therapy: ROS generation, mechanism and detection methods. Photodiagnosis and Photodynamic Therapy, 13, 40–50. https://doi.org/10.1016/j.pdpdt.2015.10.005

[66] Kruspe, S., Meyer, C., & Hahn, U. (2014). Chlorin e6 conjugated interleukin-6 receptor aptamers selectively kill target cells upon irradiation. Molecular Therapy - Nucleic Acids, 3(1), e143. https://doi.org/10.1038/mtna.2013.70

[67] Hak, A., Ali, M. S., Sankaranarayanan, S. A., Shinde, V. R., & Rengan, A. K. (2023). Chlorin e6: A promising photosensitizer in photo-based cancer nanomedicine. ACS Applied Bio Materials. https://doi.org/10.1021/acsabm.3c00407

[68] Careta, O., Compagnone, D., & Merkoci, A. (2024). Laser-assembled conductive 3D nanozyme film-based nitrocellulose sensor for real-time detection of H2O2 released from cancer cells. Biosensors and Bioelectronics, 262, 114415. https://doi.org/10.1016/j.bios.2023.114415

[69] Zhao, L., Yang, H., Amano, T., Qin, H., Zheng, L., Takahashi, A., Zhao, S., Tooyama, I., Murakami, T., & Komatsu, N. (2016). Efficient delivery of chlorin e6 into ovarian cancer cell with octalysine conjugated superparamagnetic iron oxide nanoparticle for effective photodynamic therapy. Journal of Materials Chemistry B, 4(46), 7480–7489. https://doi.org/10.1039/C6TB01988A

[70] Yu, S., Zhang, H., Zhang, S., Zhong, M., & Fan, H. (2021). Ferrite nanoparticles-based reactive oxygen species-mediated cancer therapy. Frontiers in Chemistry, 9, 712019. https://doi.org/10.3389/fchem.2021.712019

[71] Ming, L., Cheng, K., Chen, Y., Yang, R., & Chen, D. (2021). Enhancement of tumor lethality of ROS in photodynamic therapy. Cancer Medicine, 10(1), 257-268. https://doi.org/10.1002/cam4.3592

[72] Zhang, Z., Wang, Z., Xiong, Y., Wang, C., Deng, Q., Yang, T., Xu, Q., Yong, Z., Yang, X., & Li, Z. (2021). A two-pronged strategy to alleviate tumor hypoxia and potentiate photodynamic therapy by mild hyperthermia. Biomaterials Science, 9(13), 4761-4773. https://doi.org/10.1039/D1BM00444F

[73] Circu, M. L., & Aw, T. Y. (2010). Reactive oxygen species, mitochondria, and apoptosis. Free Radical Biology and Medicine, 48(6), 749–762. https://doi.org/10.1016/j.freeradbiomed.2009.12.022

[74] Luo, M., Li, H., Han, D., Yang, K., & Kan, L. (2021). Inhibition of autophagy enhances apoptosis induced by Ce6-photodynamic therapy in human colon cancer cells. Photodiagnosis and Photodynamic Therapy, 34, 102331. https://doi.org/10.1016/j.pdpdt.2021.102331

[75] Zhang, T., Lin, H., Cui, L., An, N., & Tong, R. (2016). Near infrared light triggered reactive oxygen species responsive upconversion nanoplatform for drug delivery and photodynamic therapy. European Journal of Pharmaceutics and Biopharmaceutics, 108, 161-170. https://doi.org/10.1016/j.ejpb.2016.08.002

[76] Amaroli, A., Pasquale, C., Zekiy, A., Utyuzh, A., Benedicenti, S., Signore, A., & Ravera, S. (2021). Photobiomodulation and oxidative stress: 980 nm diode laser light regulates mitochondrial activity and reactive oxygen species production. Oxidative Medicine and Cellular Longevity, 2021, 6626286. https://doi.org/10.1155/2021/6626286

[77] Zheng, X. T., Hua, W., Wang, H., Yang, H., Zhou, W., & Li, C. M. (2023). Bifunctional electro-optical nanoprobe to real-time detect local biochemical

processes in single cells. Biosensors and Bioelectronics, 222, 115070. https://doi.org/10.1016/j.bios.2023.115070

[78] Hallas-Potts, A., Dawson, J., & Herrington, C. (2019). Ovarian cancer cell lines derived from non-serous carcinomas migrate and invade more aggressively than those derived from high-grade serous carcinomas. Scientific Reports, 9, 11628. https://doi.org/10.1038/s41598-019-48179-7

Curriculum Vitae

Name Surname : Seyedeh Zeinab Mirhosseni

Education:

2014–2019	İzmir Kâtip Çelebi University, Dept. of Biomedical Eng. (BSc)
2022–2024	İzmir Kâtip Çelebi University, Dept. of Biomedical Eng (MSc)

Work Experience:

2017 Summer Internship	Takht-e Jamshid Public Hospitals Authority
2018 Summer Internship	Meditera Group Inc.